MASTER'S THESIS

Artificial Neural Networks applied to predict mechanical properties of unidirectional composites reinforced with natural fibers

Tiago Luis Santos Silva

Alagoinhas/BA

eng.tiagoluis@gmail.com

supervision of:

Dr. Genilson Cunha de Oliveira Filho

Professor at the State University of Bahia

UNEB
UNIVERSIDADE DO
ESTADO DA BAHIA

PPGMSB

Bahia State University

Department of Exact and Earth Sciences II

Postgraduate Program in Biosystems Modeling and Simulation

Tiago Luis Santos Silva

Artificial Neural Networks applied to predict mechanical properties of unidirectional composites reinforced with natural fibers

Master's thesis submitted to the State University of Bahia, in the Graduate Program in Biosystems Modeling and Simulation, as a partial requirement to obtain the title of Master in Biosystems Modeling and Simulation.

Interdisciplinary Field

Major Field: Modeling Applied to Biosystems

Research Area: Biosystems Modeling and Optimization

Advisor: Dr. Genilson Cunha de Oliveira Filho

co-advisor: Dr. Alexandre do Nascimento Silva- (UESC)

URL www.ppgmsb.uneb.br/tcc

Alagoinhas/BA

27/06/2024

APPROVAL SHEET
"ARTIFICIAL NEURAL NETWORKS APPLIED TO THE PREDICTION OF MECHANICAL PROPERTIES OF UNIDIRECTIONAL COMPOSITES REINFORCED WITH NATURAL FIBERS."

TIAGO LUIS SANTOS SILVA

Dissertation presented to the Postgraduate Program in Modeling and Simulation of Biosystems - PPGMSB, on June 27, 2024, as a partial requirement for obtaining the degree of Master in Modeling and Simulation of Biosystems from the State University of Bahia, as evaluated by the Examining Board:

Documento assinado digitalmente
gov.br **GENILSON CUNHA DE OLIVEIRA FILHO**
Data: 16/09/2024 20:47:14-0300
Verifique em https://validar.iti.gov.b

Professor Dr. GENILSON CUNHA DE OLIVEIRA FILHO UNEB

PhD in Mechanical Engineering Federal University
of Pernambuco

Documento assinado digitalmente
gov.br **ALEXANDRE DO NASCIMENTO SILVA**
Data: 09/09/2024 12:50:48-0300
Verifique em https://validar.iti.gov.br

Professor Dr. ALEXANDRE DO NASCIMENTO SILVA UNEB

PhD in Computational Modeling and Industrial Technology
SENAI - Regional Department of Bahia

Documento assinado digitalmente
gov.br **JOSE ROBERTO DE ARAUJO FONTOURA**
Data: 08/08/2024 15:46:31-0300
Verifique em https://validar.iti.gov.br

Professor Dr. JOSE ROBERTO DE ARAUJO FONTOURA UNEB
PhD in Knowledge Dissemination Federal University of Bahia

Documento assinado digitalmente
gov.br **FREDE DE OLIVEIRA CARVALHO**
Data: 28/08/2024 15:03:30-0300
Verifique em https://validar.iti.gov.br

Professor Dr. FREDE DE OLIVEIRA CARVALHOUFAL
PhD in Chemical Engineering State University of Campinas

Dedication

I dedicate this work firstly to my family, then to everyone who directly and indirectly contributes to the completion of this new stage of my professional life.

ABSTRACT

This work aims to apply artificial neural network (ANN) models for the analysis of properties of a unidirectional composite reinforced with natural fibers, thus providing theoretical values of mechanical properties such as the transverse elasticity modulus of the composite. Furthermore, with these obtained values, establishing a relationship with the Halpin-Tsai model, through the correlation coefficient and mean square error. To do so, it was necessary to use a dataset that was divided into two parts, one part being used for training and the other for ANN testing. For this work, three different network architectures were developed: one with only two inputs, another with three inputs, and the last consisting of a hybrid architecture that combines an ANN with a model developed by Halpin-Tsai. After training the algorithms, the results demonstrate that the use of ANN is quite promising, as the results of the hybrid model (ANN/Halpin-Tsai) show higher correlation coefficient values and lower mean square error values. While the ANN with two inputs failed in modeling, the one with three inputs showed positive results compared to the Halpin-Tsai model. The effectiveness of the hybrid model lies in its ability to generalize, combining the ANN and the Halpin-Tsai data.

Keywords: Natural Fibers, Unidirectional Composites, Transverse Elasticity Modulus, Halpin-Tsai Model, Artificial Neural Network (ANN).

List of Acronyms

E_2 - Transverse Elasticity Modulus

E_1 - Longitudinal Elasticity Modulus

E_f - Fiber Elasticity Modulus

E_m - Matrix Elasticity Modulus

G_{12} - Shear Modulus

$\sigma_{c,l}^*$ - Composite Strength Limit in the Longitudinal Direction

X_t - Ultimate Longitudinal Tensile Strength

m_c - Composite Mass

m_f - Fiber Mass

m_m - Matrix Mass

M_c - Composite Mass Fraction

M_f - Fiber Mass Fraction

M_m - Matrix Mass Fraction

M - Mass Fraction

r - Correlation Coefficient

V_c - Composite Volume Fraction

V_f - Fiber Volume Fraction

V_m - Matrix Volume Fraction

V_v - Void Volume Fraction

$\nu_{\mathbf{12}}$ - Major Poisson's Ratio

ν_{21} - Minor Poisson's Ratio

ν_{23} - Poisson's Ratio in Direction 23

$E_{f\,max}$ - Maximum Fiber Elasticity Modulus

$E_{m\,max}$ - Maximum Matrix Elasticity Modulus

$E_{2\,max}$ - Maximum Transverse Elasticity Modulus

$E_{f\,min}$ - Minimum Fiber Elasticity Modulus

$E_{m\,min}$ - Minimum Matrix Elasticity Modulus

$E_{2\,min}$ - Minimum Transverse Elasticity Modulus

$E_{f\,nor}$ - Normalized Fiber Elasticity Modulus

$E_{m\,nor}$ - Normalized Matrix Elasticity Modulus

$E_{2\,nor}$ - Normalized Transverse Elasticity Modulus

$E_{2\,real}$ - Transverse Elasticity Modulus obtained Experimentally

$E_{2\,rna}$ - Transverse Elasticity Modulus of the Artificial Neural Network

$E_{2\,estimado}$ - Transverse Elasticity Modulus obtained by Halpin-Tsai Equations

ΔW - Variation of Synaptic Weights

ζ - Geometric Parameter

List of Abbreviations

NN Neural Network

ANN Artificial Neural Network

MSE Mean Squared Error

MLP *Multilayer Perceptron*

RPROP Resilient Backpropagation

List of Figures

List of Tables

Summary

Introduction

In the field of mechanical engineering, the need to improve materials with properties aimed at reducing environmental impact has become increasingly essential, allowing them to meet new requirements for industrial applications.

In this context, the incorporation of natural fibers into unidirectional composites has gained prominence, offering not only a sustainable alternative, but also improving properties such as tensile strength and stiffness, compared to conventional composites made solely with synthetic fibers. This approach shows potential to meet industry demands by providing more ecologically sustainable solutions.

Furthermore, unidirectional composites stand out as a class of materials capable of achieving such objectives and have been widely used in industries due to their ability to satisfy these needs. These materials exhibit complex mechanical properties, often requiring a level of investment that may not align with the cost-benefit ratio of the experiments needed to obtain the desired information (Lorandi, Cioffi, & Ornaghi Jr, 2016).

However, these mechanical properties are essential for failure analysis and the design of structural components. Thus, several mathematical models have been proposed to describe the behavior of these materials, aiming to reduce the number of required tests, predict results, and ultimately lower project costs (Callister & Rethwisch, 2020).

The mathematical models used to analyze the mechanical behavior of unidirectional composites based on their components are known as micromechanical models. These models seek to obtain the properties of the composite based on the individual properties of its components and the volume fractions of each element (Vasiliev & Morozov, 2001).

In the literature, there are several mathematical, empirical, and semi-empirical models used to estimate the elastic properties of composite materials based on the individual properties of their components. The simplest of these is known as the "rule of mixtures". One widely used model today is the Halpin-Tsai model (Vasiliev & Morozov, 2001).

These models provide a simplified approach for predicting elastic properties, taking into account factors such as the volume fraction of the components, their intrinsic properties, and the interactions between them.

The Artificial Neural Network (ANN) is a modern computational tool widely adopted in various engineering fields, including mechanical engineering. These networks are inspired by the functioning of the human brain and rely on mathematical models that enable computational learning from a set of predefined data, acquiring knowledge through experience in computational training (Haykin, 2001).

These basic units, called neurons or processors, are interconnected, forming a complex network of connections, hence the name "neural networks". This network structure makes it possible to perform a wide range of tasks, being especially effective as a universal function approximator (Júnior, Neto, & de Aquino, 2005).

In the field of composite materials, neural networks are already being applied, showing promising results.

1.1 Research Problem

Laboratory experiments aimed at investigating the mechanical behavior of unidirectional composite materials with natural fibers face significant challenges due to the low isotropic level and high hydrophilic capacity of natural fibers, in addition to the complexities at the fiber-matrix interface.

How can the mechanical behavior of unidirectional composite materials with natural fibers be anticipated, considering the challenges associated with the fibers' low isotropic level, high hydrophilic capacity, and the complexities at the fiber-matrix interface?

1.2 Objectives

General Objective

Apply ANN models to analyze the properties of a unidirectional composite reinforced with natural fibers, in order to provide theoretical values for mechanical properties, such as the transverse modulus of elasticity of the composite. Additionally, establish a relationship with the Halpin-Tsai model by using the correlation coefficient (r) and the Mean Squared Error (MSE) to compare the values obtained.

Specific Objectives

- Develop a model for the transverse modulus of elasticity based on the mechanical behavior of unidirectional structural composite materials reinforced with natural fibers, using three distinct architectures.

- Apply analytical models to analyze mechanical properties, with a focus on the Halpin-Tsai model.

- Evaluate the results obtained from the analytical models and ANN in order to validate the algorithm's effectiveness. The comparative analysis will be conducted both qualitatively, through graphical representation, and quantitatively, using MSE and the correlation coefficient (r).

1.3 Justification

The growing demand for innovations in mechanical engineering and the constant improvement of unidirectional composite materials require efficient approaches to predict mechanical properties accurately and cost-effectively. In this context, the use of ANN appears as a promising strategy, taking advantage of the ability of these models to learn complex patterns from datasets (Diniz et al., 2016).

The need to predict mechanical properties in unidirectional composites drives the use of ANN, which offer accuracy and efficiency even in complex scenarios. Furthermore, the integration of natural fibers promotes environmental sustainability in the composite materials industry.

Unidirectional composites present specific challenges, such as the need to predict complex mechanical properties, including the transverse modulus of elasticity (E_2), in scenarios where traditional methods can be expensive and require a significant amount of experimental tests. ANN, by simulating human learning, offers the advantage of generalization and prediction capacity, even in situations where the relationships between variables are intricate (Watt, Davies, & O'Connell, 1976).

The application of ANN in the micromechanics of unidirectional composites provides an opportunity for advancement in computational modeling, allowing the simplification of processes and reducing dependence on traditional models, such as the mixture rule and the Halpin-Tsai model. Furthermore, the flexibility inherent to ANN allows the exploration of different architectures and training algorithms, adapting to the specificities of unidirectional composites (Goleman, 2017).

1.4 Motivation

The use of natural fibers in unidirectional composites not only presents mechanical benefits, but also brings significant considerations from an ecological point of view. Natural fibers are renewable, biodegradable resources and generally have a lower environmental impact compared to traditional synthetic fibers (Romão, 2003).

The need to anticipate the mechanical behavior of these materials, such as the transverse modulus of elasticity (E_2), is crucial to optimize industrial projects and processes. The difficulty lies not only in the diversity and specificity of mechanical properties, but also in the high demand for resources associated with traditional experimentation.

Neural Network (NN)'s approach offers a promising perspective, inspired by human learning, to overcome these challenges. The ability of these models to learn patterns from complex data allows for more accurate prediction, reducing dependence on a purely experimental approach. By simulating the cognitive process, ANN can capture non-linear and complex relationships, offering a valuable alternative for modeling unidirectional composites.

The flexibility of ANN, combined with its generalization capacity, offers a unique opportunity to optimize the analysis of unidirectional composites, aligning with the growing demands for more agile and effective methods in modern mechanical engineering.

Therefore, by including unidirectional composites reinforced with natural fibers, not only does it advance the efficiency and precision of mechanical engineering, but it also contributes to mitigating environmental impacts and promoting more sustainable practices in industry.

1.5 Questions and hypotheses

Based on the ANN responsible for predicting the transversal modulus of elasticity of unidirectional composites reinforced with natural fibers, some questions can be raised:

- How can ANN be applied to predict the mechanical behavior of unidirectional composites with natural fibers, overcoming the challenges related to the low isotropic level and high hydrophilic capacity of these fibers?

- What are the specific characteristics of neural architectures that best adapt to the analysis of unidirectional composites, considering the simplification of the model through a reduced number of input parameters?

To support an argument on these issues, the following hypotheses are outlined:

- The use of properly trained ANN can overcome the difficulties related to the low isotropic level and high hydrophilic capacity of natural fibers, providing a more accurate prediction of the mechanical behavior of unidirectional composites;

- Simplified neural architectures, which seek to adapt to micromechanical principles, with a reduced number of input parameters, will present satisfactory performance in the prediction of mechanical properties, equivalent to conventional models, such as the Halpin-Tsai model;

1.6 Delimitation of the study

This study will be restricted to the application of ANN in the prediction of the transverse modulus of elasticity (E_2) in unidirectional composites. The delimitation includes the specific analysis of these materials, considering their unidirectional fiber orientation, and the emphasis will be on the mechanical properties. The delimitation excludes other types of materials, such as bidirectional, multidirectional and randomly oriented composites. The comparative evaluation will be performed quantitatively, using metrics such as MSE and the correlation coefficient (r), and qualitatively, through graphs. This study focuses on the practical application of ANN in mechanical engineering, specifically to predict mechanical properties in unidirectional composites.

1.7   Relevance of the study

This study seeks to explore and improve methods for predicting mechanical properties in unidirectional composites, with the aim of simplifying these processes, allowing for a more accurate and cost-effective prediction of the transverse modulus of elasticity (E_2) through the use of NN. Furthermore, by considering unidirectional composites reinforced with natural fibers, the study expands the applicability of the techniques developed to more sustainable materials with lower environmental impact.

Reducing experimental costs is a significant consideration, as the study proposes an efficient alternative to the traditional approach, reducing the need for experimental testing, especially in scenarios where conventional methods may be economically unfeasible. By incorporating unidirectional composites reinforced with natural fibers, the research can also contribute to reducing costs associated with the acquisition and processing of materials, promoting more sustainable and economically viable practices.

This approach has the potential to generate knowledge directly applicable to structural projects, while promoting the adoption of more sustainable materials in the industry.

The potential for generalization is a strategic dimension, since the results obtained are not limited to unidirectional composites, and can be extended to a broader application of ANN in other contexts in materials engineering.

Composite Materials

Composite materials are materials made by combining two or more components with different properties, usually a matrix material and a reinforcing material. This combination results in a material that has superior properties to those of the individual materials, making them widely used in various industries, including aerospace, automotive, construction, sports, and electronics, among others (Callister & Rethwisch, 2020).

They have properties that could hardly be achieved by conventional materials, being composed of metals, ceramics and polymers. This diversity of materials allows them to achieve performance levels that no individual material could offer, making them ideal for meeting the demands of these applications mentioned.

2.1   Classification of Composite Materials

Composite materials have characteristics that are very different from other types of materials, and these characteristics are correlated to their composition, orientation of the reinforcing fibers and their geometry (Callister & Rethwisch, 2020).

Reinforcements are the components that provide greater strength to composites. They are generally referred to as the dispersed phase and play a fundamental role in transporting the load in composite materials, providing greater strength, modulus and elasticity. Synthetic fibers are the most common type of reinforcement and are mostly produced from petroleum-derived resins. Some of the main fibers used as reinforcement in composite materials are: carbon, polyethylene, polypropylene, glass, nylon and aramid (Oliveira, 2018).

Microcomposite materials are subdivided into four categories: fibrous composite materials, particulate composite materials, laminated composite materials and hybrid composite materials. However, for the purposes of this work, only fibrous composite materials are relevant.

In Figure 2.1, an example of a multilayer composite with multiple orientations of the reinforcing fibers can be seen.

Figura 2.1: Example of Multi-Layer Composite.
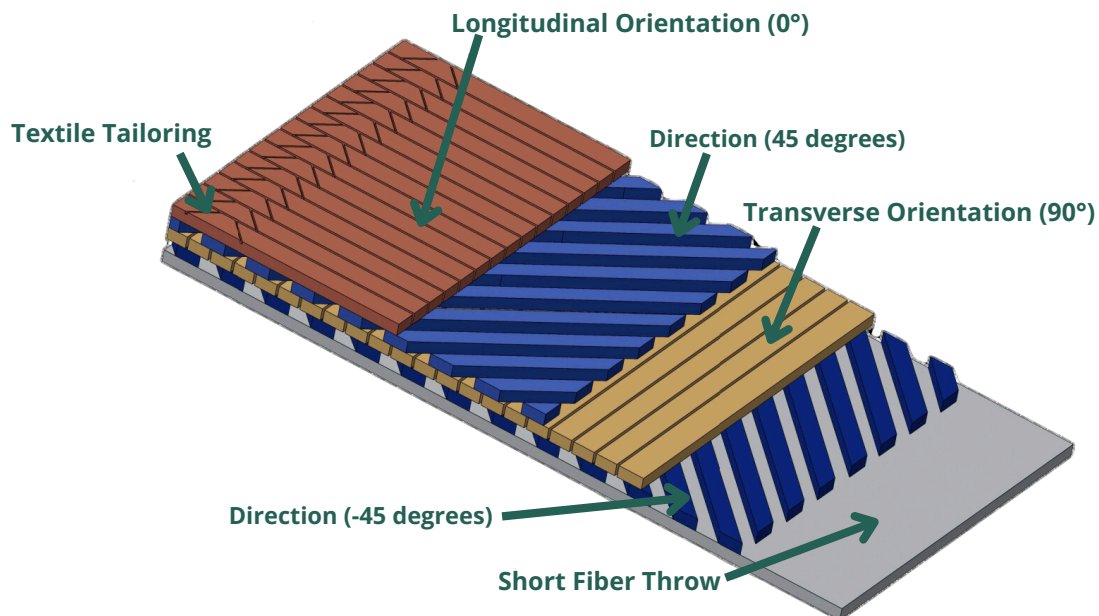
Source: Prepared by the author (2024).

Fibrous Composite Materials

The fibrous reinforcement of a composite material consists of thousands of individual filaments with very small diameters of the order of micrometers, dispersed in the polymer matrix. Typically, the mechanical properties of the fibers are much higher than those of the polymer they reinforce (Bank, 2006).

In addition to these requirements, which are demanded of the matrices, the fibers must also have characteristics that allow them to reinforce the polymers effectively (Romão, 2003).

In addition to the requirements mentioned above, there are other factors related to the nature of the reinforcement that influence the final properties of a composite. The quantity of fibers, their orientation and their length are characteristics that predominantly influence the characteristics of fiber-reinforced polymers, so much so that the composites can be classified according to the scheme in Figure 2.2.

Figura 2.2: Possible ways of using fibers in the manufacture of composite materials.

Bidirectional Fabric

Blanket with continuous threads

Unidirectional Fabric

Blanket with short threads
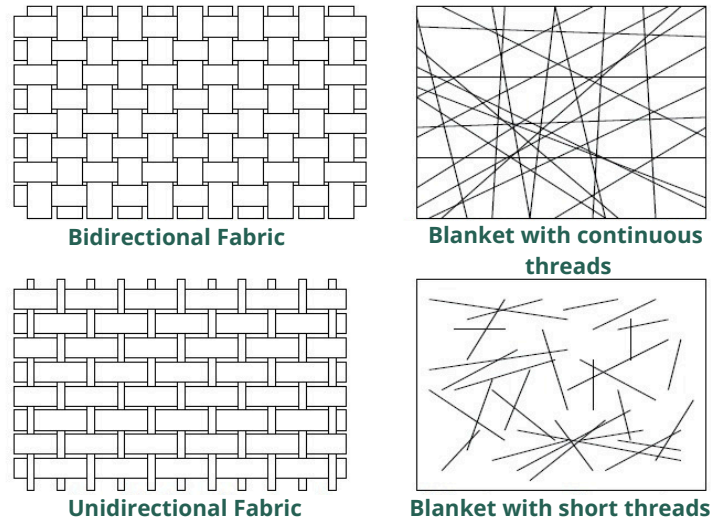
Source: Adapted from Kaw (2005).

2.2   Natural fibers

Since the dawn of humanity, natural fibers have been used to improve the properties of materials. As an example of the first fibers of natural origin used, linen has a history of over 8 thousand years, having originated in Egypt, on the banks of the Nile, and in Crimea, as confirmed by archaeological findings. Cotton is also an example of a very old natural fiber. The time when man began to cultivate cotton for textile purposes is still uncertain. In India, traces of this woven fiber can be found dating back to 3200 BC, as well as signs of remote cotton plantations (Pezzolo, 2019).

In Brazil, different types of fibers can be cited, which have distinctions in their mechanical, chemical and physical properties.

Natural fibers such as cotton, sisal, jute, hemp, or linen are renewable in nature, cheaper, and have a lower environmental impact, since they are biodegradable. Replacing parts reinforced with synthetic fibers with those reinforced with natural fibers is highly recommended, as it reduces the possible environmental impacts inherent to synthetic materials (Romão, 2003).

Some benefits that can be observed with its use include low thermal conductivity, high electrical resistance and the ability to increase diffusion, making it suitable as an acoustic material. In addition, the lower weight of composites reinforced with natural fibers improves fuel efficiency. Compared to other synthetic fibers, it has a low specific density and offers a good cost-benefit ratio (Schelb, 2016).

However, there are also possible limitations arising from the use of natural fibers as reinforcement of polymeric materials, such as low temperature resistance, high hydrophilic affinity and lack of interface between the fibers and the matrices. The biggest problem related to natural fibers is due to the hydrophilic groups present in their chemical structure. These groups give natural fibers a polar property, while olefinic polymers are nonpolar.

Classification of Natural Fibers of Plant Origin.

Natural fibers are subdivided according to their origin: vegetable, animal or mineral. Due to their properties, fibers of vegetable origin have greater potential in engineering, as can be seen in Figure 2.3.

Figura 2.3: Diagram of the classifications of natural fibers of plant origin.
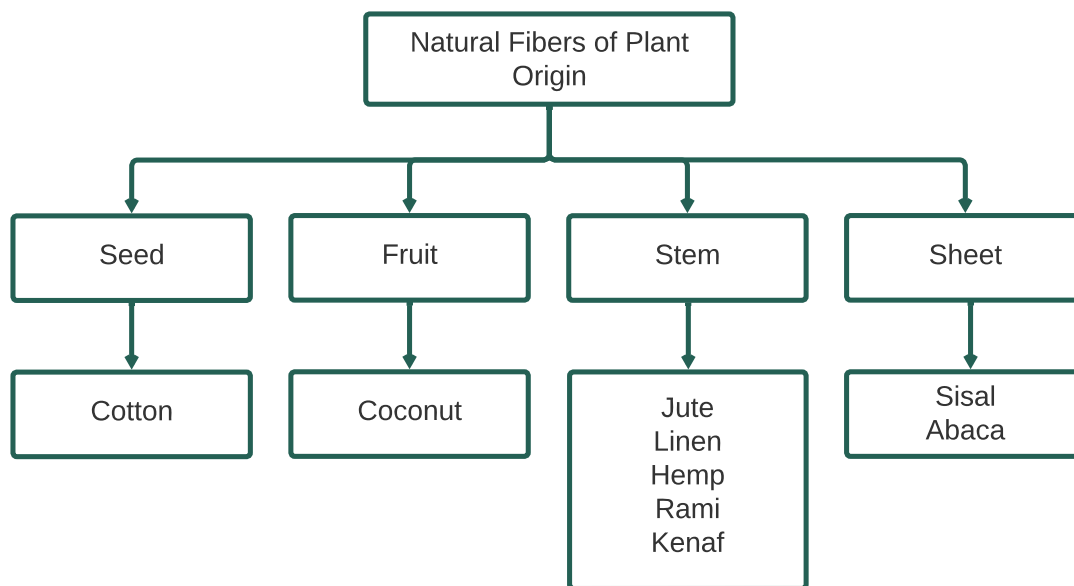
Source: Adapted from Faruk, Bledzki, Fink, and Sain (2012).

For example, fibers of animal origin have lower resistance and greater elongation in relation to vegetable fibers, while mineral fibers have a higher purchasing value, are more brittle and lack resistance and flexibility (Castro, 2013).

Structure and Constituents of Natural Fibers of Plant Origin.

Their characteristics depend on the properties of the individual constituents, the fibrillar structure and the lamellar matrix. The fiber is composed of numerous elongated spindle-shaped fiber cells that taper towards each end. Therefore, all plant fibers are hydrophilic in nature; their moisture content reaches 8-13% (Castro, 2013).

Natural fibers of plant origin contain different natural substances. The most important of these is lignin. The distinct cells of hard plant fibers are joined together by lignin, which acts as a cementing material. The lignin content of plant fibers influences their structure, properties, and morphology (Araújo, 2019).

Considered as naturally occurring composites, they are composed mainly of cellulose fibrils embedded in a lignin matrix. These cellulose fibrils are aligned along the length of the fiber. It appears that this alignment provides maximum tensile and flexural strength, in addition to providing rigidity in this direction of the fiber, as can be seen in Figure 2.4 (Nascimento, Silva, Dias, Gomes, & Fujiyama, 2019).

Figura 2.4: Structural constitution of a vegetable fiber.
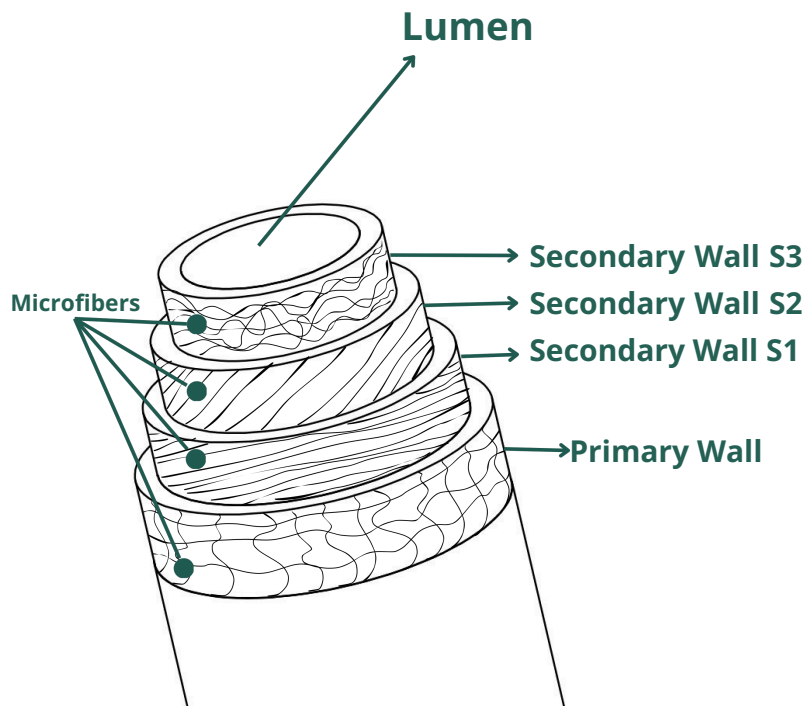
Source: Adapted from Eichhorn, Hearle, Jaffe, and Kikutani (2009).

For each type of natural fiber, the percentage of the four main chemical constituents is presented, as can be seen in Table 2.1.

2.3 Matrix

The matrix used in the manufacture of composite materials aims to transfer mechanical loads to the reinforcement, giving its structure ductility and cohesion. By involving the reinforcement material, it provides flexibility to the composite, while protecting it against the influences of the external environment (A. P. d. O. Silva, Quaresma, Motta, & Francklin, 2015).

Tabela 2.1: Chemical constituent contents of some natural fibers of plant origin.

Origin	Fibers	Cellulose (%)	Hemicellulose (%)	Lignin (%)	Pectin (%)
Seed	Cotton	82-96	2-6.4	0-5	<1-7
Fruit	Coconut	43-46	0.25	45-46	3-4
Stem	Jute	51-84	12-20	5-13	0.2
Stem	Flax	60-81	14-20.6	2.2-5	1-4
Stem	Hemp	70-92	18-22	3-5	1
Stem	Ramie	68-76	13-15	0.6-1	2
Stem	Kenaf	44-87	22	15-19	2
Leaf	Sisal	43-78	10-24	4-12	0.8-2
Leaf	Abaca	61-64	21	12	0.8

Source: Mwaikambo (2006).

The most common types of matrices are: metallic, ceramic and polymeric, with polymeric matrices being the most used in composites. They can be divided into thermoplastic and thermoset, as can be seen in Figure 2.5.

Figura 2.5: Examples of thermoplastic and thermosetting polymer matrices.
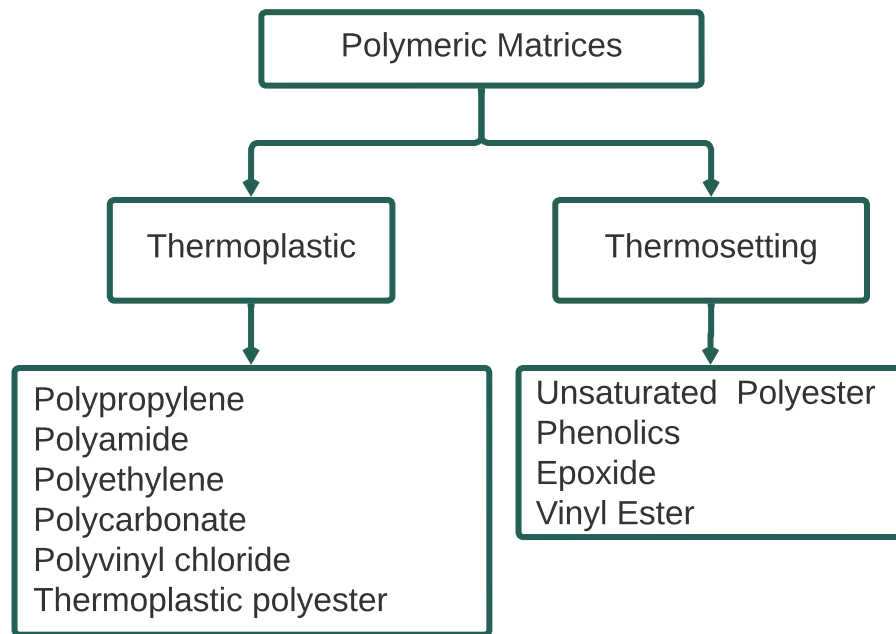
Source: Adapted from Castro (2013).

Thermoplastics are composed of macromolecules held together by relatively weak forces, such as Van der Waals forces. When heated, they become flexible due to the breaking of intermolecular bonds, reaching a viscous liquid state above the glass transition temperature. This temperature is defined as the average of the temperature range between the base line when the material is rigid and the base line when it is softened, also known as the rubbery state (Passatore, 2013).

Thermoplastics include polyethylene, polyvinyl chloride, polystyrene, polyamide, cellulose acetate, polycarbonate and polypropylene. They have the important characteristic of returning to the solid state when cooled, which allows repeated heating and cooling cycles, and are used in various manufacturing processes (Cavalcante, 2018).

On the other hand, thermosets, unlike thermoplastics, cannot be remelted and shaped repeatedly, due to the strong covalent bond between the chains. Their production occurs through a two-stage chemical reaction. The first stage results in the formation of long-chain molecules similar to those of thermoplastics, but still reactive (Vasconcelos, 2013).

In the second stage of the reaction, cross-links are formed between the chains formed in the first stage, usually through the addition of curing agents and the application of heat and/or pressure (Godoy, 2019).

2.4 Unidirectional Composite Laminates

Unidirectional composite laminates are composed of several superimposed unidirectional layers. These materials consist of two elements: the matrix and the reinforcement, with the reinforcement being formed by fibers aligned in a single direction. The complexity of the mechanical behavior of these materials is significantly greater compared to other conventional materials. Their main characteristic is the alignment of the reinforcement layers, which must all be oriented in a single direction, generally parallel to the longitudinal load (Callister & Rethwisch, 2020).

Figura 2.6: Unidirectional laminate with the main directions indicated by axes 1, 2, and 3.
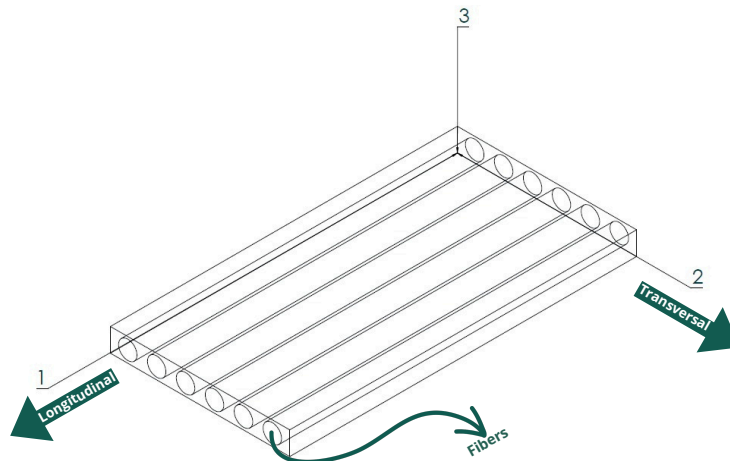
Source: Prepared by the author (2024).

In Figure 2.6, the three main axes that determine the mechanical properties of the material are identified. The reinforcement phase is composed of wires, whose layer thickness, minimum in

modern composites, is about 0.1 mm, much larger than the diameter of the fibers, which is in the range of 0.01 mm. Both the reinforcement and the matrix have their quantities specified in terms of volume and mass fractions (Vasiliev & Morozov, 2001).

2.5 Mass and Volume Fractions of a Blade

In composite materials, the quantities of fiber and matrix are expressed in volumetric and mass fractions, thus expressed by the equations 2.1 e 2.2:

$$V_f = \frac{V_f}{V_C} \quad V_m = \frac{V_m}{V_C} \quad V_v = \frac{V_v}{V_C} \tag{2.1}$$

In Equation 2.1 there is a ratio that predicts the value of the volumetric fraction of the blade components, with the term V being the volume, where the subscripts f, m, v and c indicate the values for fiber, matrix, voids and composite.

$$M_f = \frac{m_f}{m_C} \quad M_m = \frac{m_m}{m_C} \tag{2.2}$$

Likewise, Equation 2.2 is a ratio that relates the masses (m_f,m_m) of the fiber and matrix to the total m_c of the composite material, indicating their mass fractions M. Another alternative to obtain the mass fraction of the fiber and matrix is through the density of their components, as can be seen in Equation 2.3 and 2.4:

$$V_f = \left(\frac{\rho_f}{\rho_c}\right) V_f \tag{2.3}$$

$$V_m = \left(\frac{\rho_m}{\rho_c}\right) V_m \tag{2.4}$$

2.6 Damage Mechanisms

Composite materials can present a variety of damages before breaking. To describe this damage, three scales are observed: macroscale, which considers the general behavior of the laminated composite evaluated; mesoscale, which defines the laminate and the associated interface; and microscale, which considers the heterogeneous structure (Oliveira, 2018).

In the microstructure, which involves the fiber/matrix interaction, fiber fracture occurs, which can result in matrix fracture, displacement between matrix and fiber, and even fiber buckling. Mechanically, damage can lead to matrix or fiber rupture, delamination, and transverse rupture

of the sheet or laminate, which can occur independently or due to the fiber/matrix interface (Neto & Pardini, 2016).

According to Oliveira (2018), the main types of damage in composites are matrix cracking, which is characterized by one or more cracks in the matrix of the composite material, also known as cohesive fracture in the matrix; fiber rupture, which involves transverse and longitudinal rupture of the fiber, also called cohesive fracture in the fiber; and fiber/matrix debonding, which consists of displacement or detachment at the interface between fiber and matrix, called adhesive fracture.

Damage mechanisms can be influenced by several factors, such as the physical and chemical properties of the reinforcements and matrix, the composite configuration, the manufacturing process, the type of loading, the microstructural characteristics and the environmental conditions (M. A. Leão, 2013).

Delamination, which occurs due to the separation of the layers due to the degradation of the adhesive bond, can be accelerated by factors such as humidity, causing cracks and wear in certain materials. This process is more common in laminated composites. Fractures and damage can occur under various types of loads, with microbuckling restricted to compressive loads (Líbano, da Costa Pereira, Bastos, de Souza Coelho, et al., 2020).

In the case of fatigue in fibrous composites, four stages are considered: localized damage nucleation by cyclic loading, microcrack nucleation, stable crack propagation due to cyclic loading and local crack propagation, dependent on fiber orientation, matrix ductility and interface adhesion. Compressive stresses do not promote crack propagation, while tensile stresses are responsible for this phenomenon (J. F. A. Leão, 2018).

The set of structures and damage mechanisms that occur during the loading of composite materials is not fully understood, and there are several theories on the subject, especially when it comes to composites with vegetable fibers and their effects, such as moisture absorption (Recicar, 2022).

Macroscopic Analysis of the Damage Mechanism

Macroscopic analysis of damage mechanisms in materials is crucial to understanding their structural integrity and performance over time. There are at least two main forms of damage: those caused by time of use, such as wear of the material in aggressive environments, and those caused by the application of external loads, leading to mechanical fracture of the structural elements (Felipe, 2012).

In this macroscopic analysis, it is possible to observe specific damage characteristics in the specimens in mechanical tests. These characteristics may include microcracks in the material

matrix, fiber rupture, and even delamination, which is characterized by the separation of the interfaces in a laminate.

Understanding these macroscopic damage mechanisms is essential to develop maintenance, repair, and optimization strategies for materials (Oliveira, 2018).

Microscopic Analysis of Damage Mechanism

Microscopic analysis of the damage mechanism is a more detailed approach that allows investigating the fundamental causes behind material failures. While macroscopic analysis focuses on the visible effects of failures, such as fractures and wear, microscopic analysis seeks to understand the processes that occur in the microstructural (Felipe, 2012).

Figure 2.7 represents the cohesive fracture of synthetic glass fiber, while Figure 2.8 characterizes the cohesive fracture of natural sisal fiber.

Figura 2.7: Breakage of fiberglass in polymer composite.
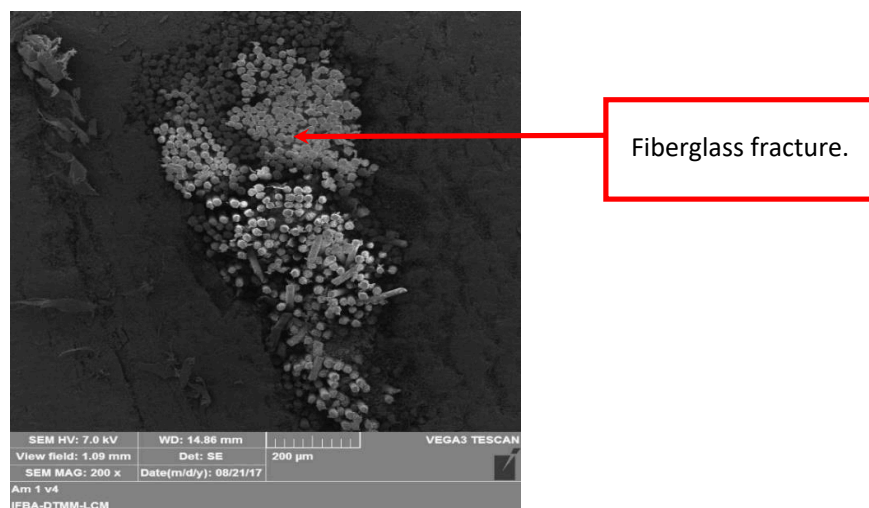
Source: Oliveira (2018).

Figure 2.9 illustrates the damage observed in polymer composites, providing examples that corroborate the theory discussed in the theoretical framework on damage mechanisms in micrographs.

2.7 Micromechanics Analysis of the Transverse Modulus of Elasticity

The equations of this approach were generally developed from the adjustment of curves with experimental data, and are considered semi-empirical because the variables involved have physical meaning. In this context, the geometry of the cross-section of the fiber analyzed

Figura 2.8: Characteristic breakage of natural fiber in polymer composite.
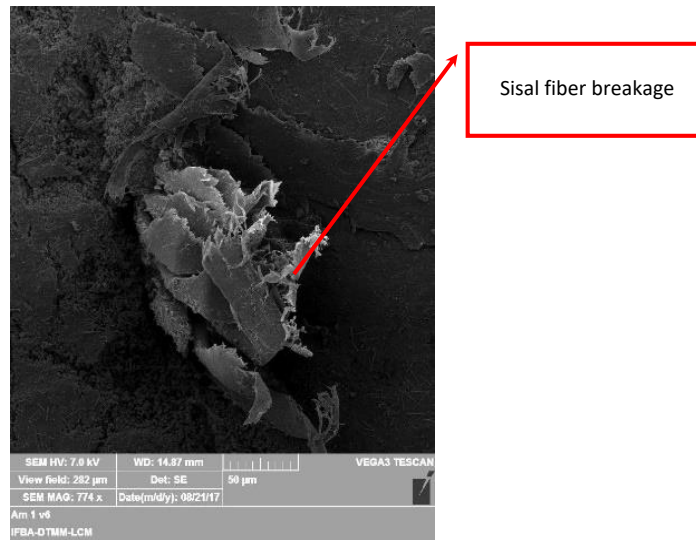
Source: Oliveira (2018).

Figura 2.9: Various examples of damages.
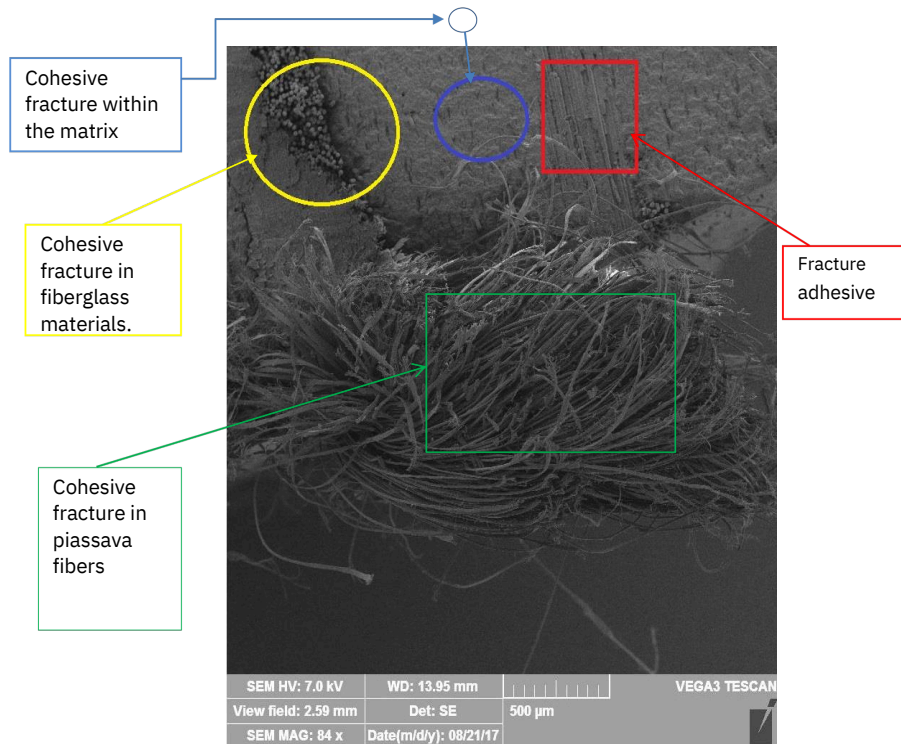
Source: Oliveira (2018).

must also be defined, since some properties are evaluated differently for rectangular and circular/square fibers (Kaw, 2005).

Rule of Mixtures

Figura 2.10: First-order model of a unidirectional laminate.
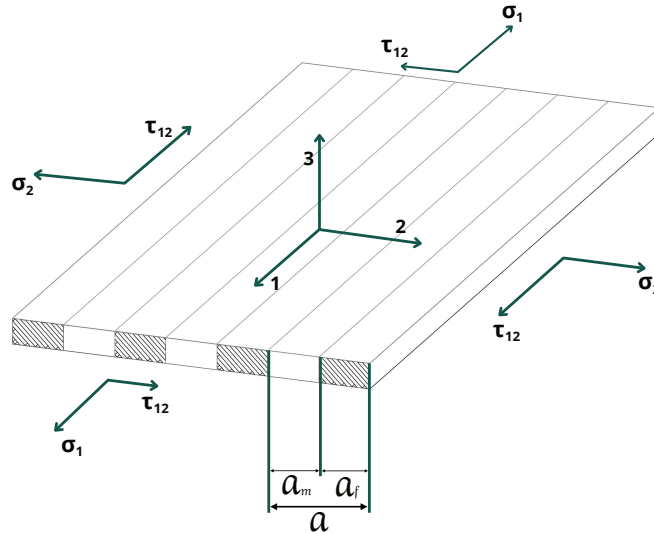
In Figure 2.10, the rule of mixtures model can be seen, also called the first-order model. This model requires the properties of the fiber and matrix, as well as the volume fraction of fibers. The diagram of this model with the blade consisting of fiber and matrix, with the respective stresses σ_1, σ_2 and σ_{12} (de Mendonça, 2005).

According to Vasiliev and Morozov (2001), the resulting force, which results in the product σ_{1a}, is distributed between the fiber and matrix strips, and the longitudinal deformation in the 1 direction is the same in these strips and in the blade as a whole. Using this modeling, it is possible to obtain some mechanical properties of composite materials, such as the longitudinal (E_1) and transverse (E_2) modulus of elasticity, Poisson's ratio ($\nu_{\mathbf{12}}$) and the composite's resistance limit in the longitudinal direction ($\sigma_{c,l}^*$).

Equations 2.5, 2.6, 2.7 and 2.8 show the models, respectively:

$$E_1 = E_2 V_f + E_2 V_f \tag{2.5}$$

$$\frac{1}{E_2} = \frac{V_f}{E_f} + \frac{V_m}{E_m} \tag{2.6}$$

$$E_2 = \frac{E_m E_f}{V_m E_f + V_f E_m}$$

$$\nu_{12} = \nu_f V_f + \nu_m V_m \tag{2.7}$$

$$\sigma_{c,l}^* = \sigma_f^* V_f + \sigma_m' \left(1 - V_f\right) \tag{2.8}$$

Another important property, also obtained by the rule of mixtures, is the ultimate longitudinal tensile stress (X_t), which is defined by Equation 2.9:

$$X_t = \sigma_{ult,f} \left[V_f \left(1 - \frac{E_m}{E_f} \right) + \frac{E_m}{E_f} \right] \tag{2.9}$$

Halpin-Tsai model

Another model that is widely used for application in the design area is the model proposed by Halpin and Tsai (1969). As it is a semi-empirical model, the model is based on experimental results, using adjusted parameters, but it also has a basis in theoretical mechanics.

Equation 2.10 serves to represent the following mechanical properties: E_2, G_{12}, ν_{23} through the variable *P*. The term V_f represents the volume fraction of fiber in the unidirectional composite (Halpin & Tsai, 1969).

$$P = \frac{P_m(1 + \zeta \eta V_f)}{1 - \eta V_f} \tag{2.10}$$

The term ζ is a geometric parameter that measures the level of reinforcement in the composite. Typically $\zeta = 2$ is used for the analysis of E_2 and $\zeta = 1$ for the analysis of G_{12}, when $\zeta = 0$ the Halpin-Tsai equation equals the equation demonstrated for the rule of mixtures (Affdl & Kardos, 1976).

For the calculation of E_2 by Halpin-Tsai it is suggested to ζ :

$$\zeta = 2 \text{ para fibra de seção circular,}$$

$$\zeta = 2a/b \text{ para fibra de seção retangular}$$

Equation 2.11 defines the parameter η of Equation 2.10.

$$\eta = \frac{P_f/P_m - 1}{P_f/P_m + \xi} \tag{2.11}$$

Artificial Neural Network

According to Haykin (2001), a neural network can be defined as a massively distributed parallel processor, consisting of simple processing units, with a natural propensity to store experimental knowledge and make it available for use. Therefore, a ANN resembles the brain in two aspects: the first in which the knowledge acquired by the network through a learning process, and the second in which the connections between neurons (synaptic weights) are used to store learning.

The NN acquires knowledge through a learning process similar to what the human brain learns from experiences and incoming information, a ANN can also learn from training data. Through learning algorithms, the network is exposed to examples and patterns, adjusting the synaptic weights of connections between neurons to capture and represent the acquired knowledge (Haykin, 2001).

The connections between neurons, represented by synaptic weights, are used to store learning. Just as synapses in the human brain strengthen or weaken based on experience and learning, the connections between neurons in a ANN are adjusted to reflect knowledge gained during training. These synaptic weights encode the relationships and patterns learned by the network, allowing it to generalize and make decisions based on the available information (Freire Jr & Aquino, 2005).

In this way, a ANN resembles the brain both in the learning process and in the storage of knowledge through synaptic connections between neurons. This similarity makes ANN a powerful tool for complex data processing tasks, such as classification, pattern recognition and decision making.

3.1 Biological Neurons

This type of cell is mainly found in the cerebral cortex of animals, as in the human brain. It consists of a cell body that contains the nucleus and most of the cell's complex components, along with several branched extensions called dendrites, as can be seen in Figure 3.1 (M. Câmara, 2014).

Figura 3.1: Neurônio Biológico.
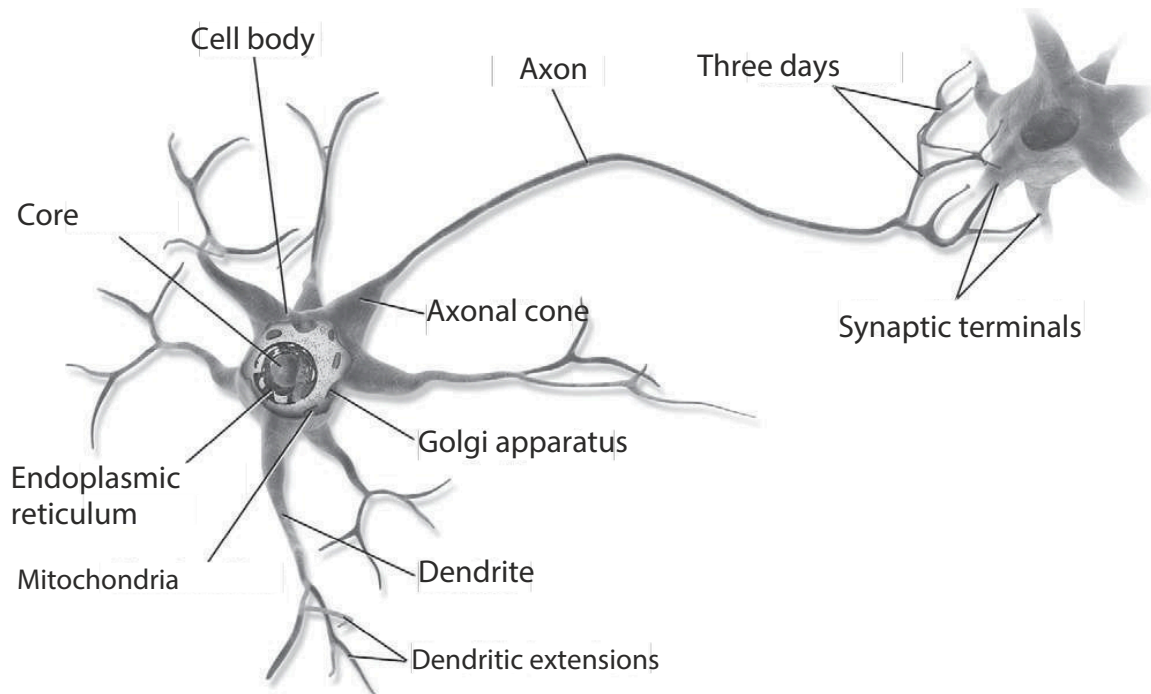
Fonte: Géron (2019).

Additionally, there is a very long extension called the axon, which may be just a few times longer than the cell body or even tens of thousands of times longer (Shepherd, 2003).

According to Shepherd (2003), near its end, the axon divides into many branches called telodendrons, and at the tips of these branches are tiny structures known as synaptic terminals, or simply synapses, which connect to the dendrites of other neurons (or directly to the cell body).

Biological neurons receive brief electrical impulses from other neurons through these synapses, called signals. When a neuron receives a sufficient number of signals from other neurons in a short space of time, it fires its own (M. Câmara, 2014) signals.

3.2   ANN neurons

Figura 3.2: Model of a Neuron.
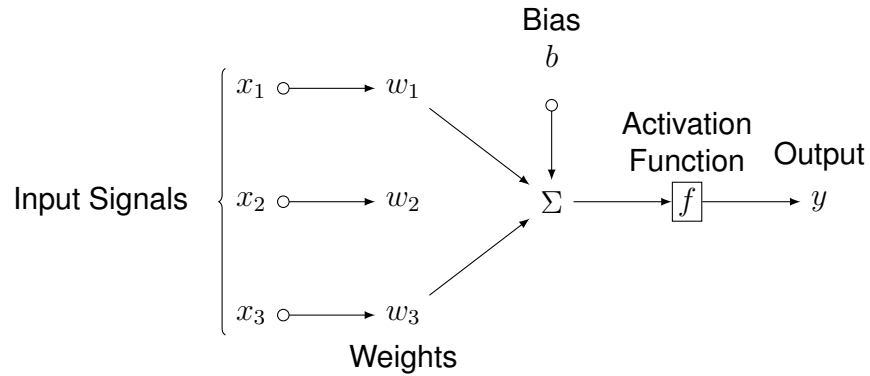
Source: Adapted from A. d. N. Silva (2017).

The fundamental cell of an artificial neural network is called a neuron, as is the case in brain neural networks. Figure 3.2 illustrates the components present within a neuron. In it, we can identify synapses, a linear combination component and an activating function (Freire Jr & Aquino, 2005).

In the artificial neural network, synapses are represented by the product of the input signals (x_n) by the corresponding weights (x_{nm}). The linear combiner performs the linear combination of synapses together with an additional element called bias (b_n), which has a specific weight. The use of bias allows more precise control of the value that will be provided to the (Júnior et al., 2005) activation function.

The activation function can adopt different forms and its main purpose is to restrict the neuron's output amplitude to a finite value. Generally, output values are limited to a specific range, such as -1 to 1 or 0 to 1. The input of the activation function corresponds to the output of the linear combiner.

The model in Figure 3.2 can be expressed by the equations 3.1 and 3.2.

$$v_n = \sum_{m=0}^{M} w_{nm}x_m + b_n w_{bn} \tag{3.1}$$

$$y_n = \varphi\left(v_n\right) \tag{3.2}$$

The term (v_n) represents the result of the sum of the linear combination of input synapses, together with the bias (b_n) multiplied by its weight (w_{bn}). The neuron's activation function is represented by φ, where y is the output of the nth neuron in the network, and M is the number of input signals.

The artificial neural network can use different types of activation functions. Among them, the sigmoid function, the hyperbolic tangent function, the threshold function and the piecewise threshold function stand out. In artificial neural network applications, the sigmoid and hyperbolic tangent functions are the most commonly used.

Figura 3.3: Sigmoid Function.
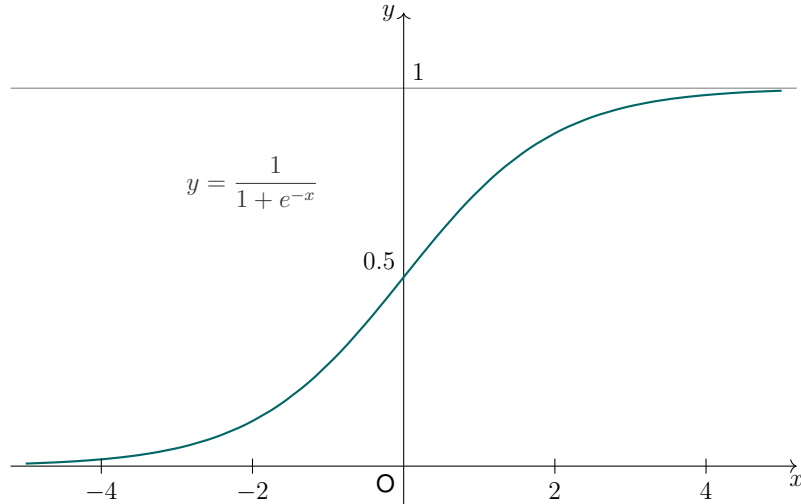
Source: Prepared by the author (2024).

The sigmoid function is defined by Equation 3.3 and its behavior is described by Figure **??**, with variation in the values of (a).

$$\varphi(x) = \frac{1}{1 + e^{-ax}} \tag{3.3}$$

The hyperbolic tangent function is defined by Equation 3.4 and its behavior is described by Figure 3.4, and the parameters (b) and (c) are constants that control the amplitude and slope of the curve.

Figura 3.4: Hyperbolic Tangent Function.
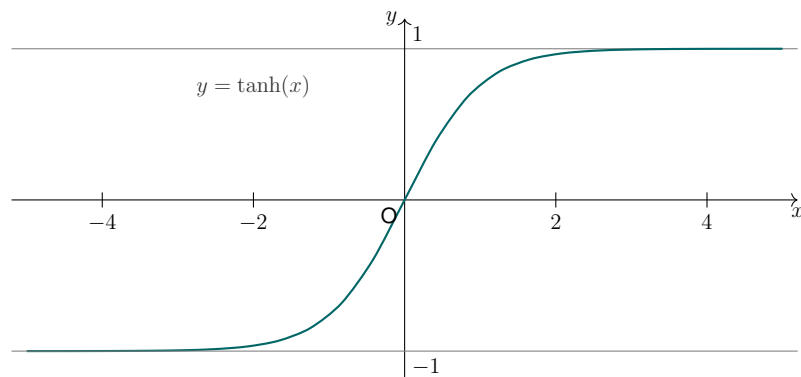
Source: Prepared by the author (2024).

$$\varphi(x) = b\tanh(cx) \tag{3.4}$$

3.3 Types of Neural Network Architecture

In the literature, there is a wide variety of neural network architectures that are applied in different types of cases. However, in this work, only the use of Multilayer Perceptron Networks will be discussed. Figure 3.5 demonstrates the type of architecture used in this research.

Figura 3.5: Multilayer perceptron network.
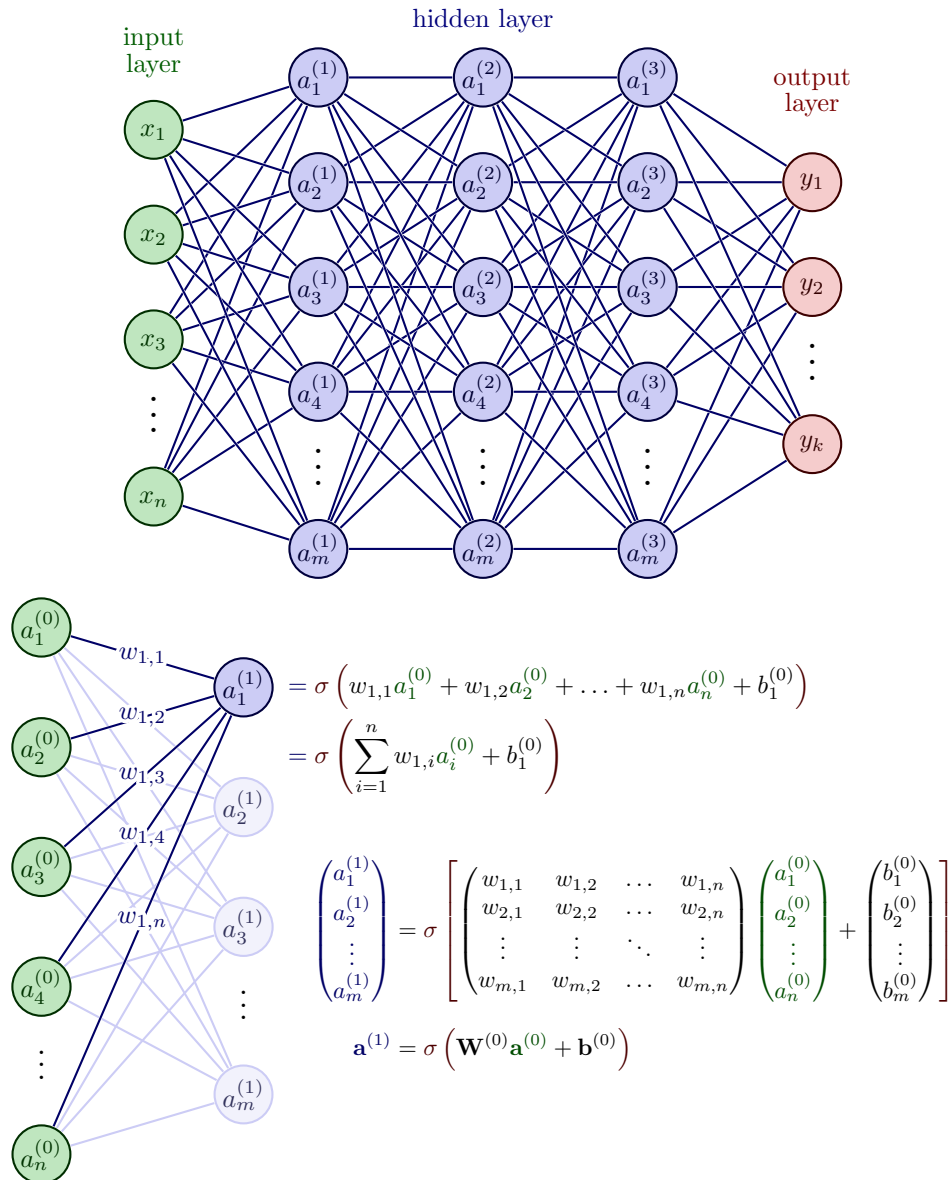
Source: Adapted from Rusell and Norvig (2013).

Perceptron de Múltiplas Camadas

A neural network *Multilayer Perceptron* (MLP) consists of an input layer, one or more hidden layers, and an output layer. Each layer is composed of neurons with multiple inputs and a single output. Each input is multiplied by an associated weight, and each output is passed through an activation function. The input signals from the neurons are propagated through the network (Haykin, 2001).

Multilayer perceptron networks have been widely used in engineering, including materials engineering. These networks have the ability to learn about a problem through training and generalize to cases not presented to the network, which makes them highly valued.

However, a disadvantage of Perceptron networks is that their operation is considered a "black box". This is due to their distributed non-linearity and the high connectivity between neurons, making theoretical analysis of their internal functioning difficult (Haykin, 2001).

As mentioned earlier, each neuron has a specific activation function, and an important characteristic is the smoothness of the sigmoid and hyperbolic tangent functions. This smoothness facilitates the calculation of their derivatives, which plays a fundamental role in the development of training algorithms for this type of architecture.

Another advantage of the sigmoid and hyperbolic tangent functions is that their derivatives are related to the primary functions themselves. This significantly simplifies the training process, reducing the number of calculations required and, consequently, decreasing the processing time during training (Haykin, 2001).

The derivative obtained from the sigmoid function is seen in Equation 3.5.

$$\frac{d\varphi(x)}{dx} = \frac{ae^{-ax}}{(1 + e^{-ax})^2} = a\varphi(x)(1 - \varphi(x)) \qquad (3.5)$$

3.4   Training a Neural Network

The characteristic that is of crucial importance for a neural network is its ability to learn, through pre-established rules and the improvement of its performance through this learning process.

The type of learning is determined by the way in which the modification of the parameters occurs. The central objective of training a neural network is to perform a gradual modification of its synaptic weights, following a learning rule that determines how these weights will be changed.

To enable learning, it is necessary to have a set of training data; during training, each time this set is presented to the network, a learning epoch occurs (Haykin, 2001).

The training algorithm is a pre-established set of well-defined rules to solve a learning problem. There are several types of training algorithms, which can be classified as supervised, semi-supervised and unsupervised. In this work, we will focus our attention only on supervised training.

Supervised Training

Supervised training aims to enable the ANN to respond approximately to the data set presented to it; in addition, it aims for the ANN to have the ability to generalize and generate approximate results for data not used in training.

Figure 3.6 illustrates a schematic of supervised training; in it, the synaptic weight matrix "w" is updated so that the ANN can model itself to the data presented in training. These changes in the "w" matrix are intended to reduce the error between the desired values ("d") and the output values ("z").

Figura 3.6: Diagrama esquemático demonstrando o processo de aprendizado de uma rede neural, aonde (a) é o método de treinamento da RNA e (b) é o modelo obtido pelo treinamento da RNA.
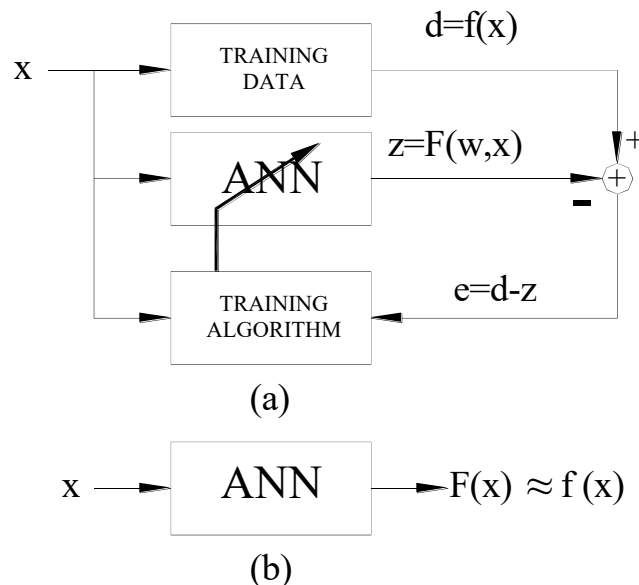
Fonte: SILVA (2001).

As mentioned earlier, there are several types of training algorithms, including Resilient Back-propagation (RPROP) (Riedmiller & Braun, 1993), Quickprop (Fahlman et al., 1988) and the most widely known, Backpropagation (Møller, 1993).

Each of these algorithms has its own particularities and is requested according to the specific application, choosing the one that best fits the characteristics of the problem in question.

Networks employing the RPROP algorithm differ from classical Backpropagation networks in that at each iteration with a specific sample size, the weights are updated in the most likely direction (Riedmiller & Braun, 1993). RPROP determines the step size for each iteration of individual weights based on the agreement or disagreement of the sign of the partial derivative with respect to the previous step. Its main advantage is the ability to adapt its learning rates to the error topology (Costa et al., 2021).

Backpropagation Algorithm

The Backpropagation algorithm requires some architectural characteristics, of which we can mention: the nonlinear activation function must have a derivative at all points, the ANN must have one or more layers of hidden neurons, and the ANN must have a high degree of connectivity. Once these characteristics are approved, the objective of the training is to reduce as much as possible the MSE, also called the cost function, which is presented in Equation 3.6.

$$MSE = \frac{1}{2Q} \sum_{1}^{Q} \sum_{p_1=1}^{P_1} (d_{p_1} - z_{p_1})^2 \qquad (3.6)$$

In order to minimize MSE, it is necessary to modify the synaptic weights and this is done by implementing the training algorithm with forward propagation and back propagation.

$\delta_i^{(L+1)}$ corresponds to the errors that are propagated back from layer $(l + 1)$ to layer (l), as can be seen in Figure 3.7.

Figura 3.7: Backpropagation in deep networks.
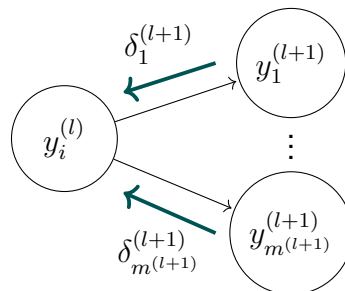
Fonte: Adaptado de Freire Jr and Aquino (2005).

These computational steps can be interpreted as signals. The functional signal travels through the network, and the error signal is provided by the training algorithm, thus modifying the internal structure of the network (synaptic weights).

The modification of the synaptic weights, through the error signal, is carried out following the rules that are obtained through the derivation of the cost function in relation to the variation given to the synaptic weights.

Figura 3.8: T-layer Perceptron Network.

In Figure 3.8, the indices l, m and n represent the neurons of a network that propagates from left to right, such that l is the neuron that is in a layer to the left of neuron m (layer before neuron m) and neuron n is in a layer to the right of this same neuron (layer after neuron).

From the rules obtained and considering a multilayer Perceptron network with "T" layers (as shown in Figure 3.8) the training of the network can be divided into 5 stages.
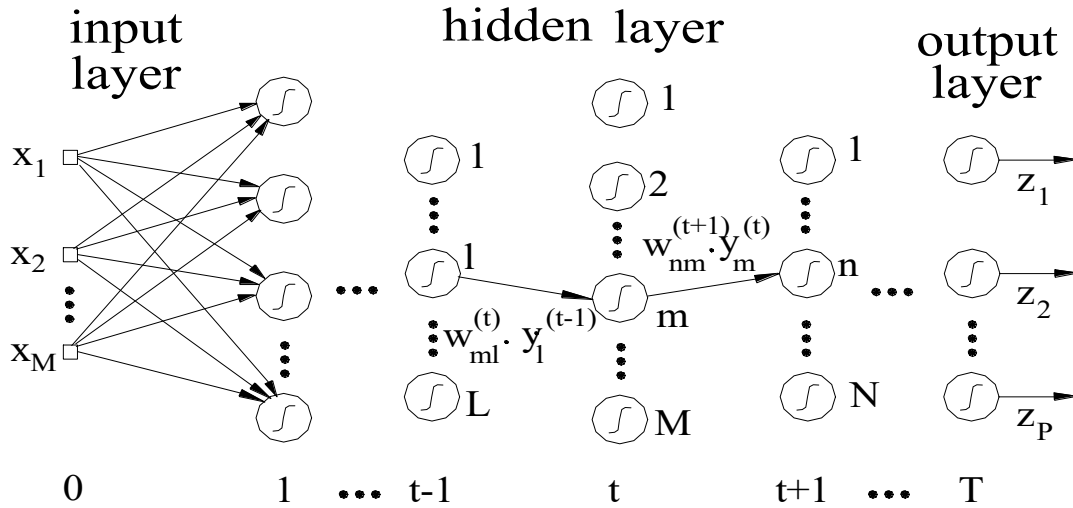
1. Start: Initially, the values of the synaptic weights must be chosen randomly, so that the mean of their values is zero and the variance is close to the saturation of the activation function used (the activation function used can be sigmoid or hyperbolic tangent).

2. Presentation of training data: An epoch of training examples is presented to the network. For each example presented, the sequences described in items 3 and 4 are performed, in which the functional signal and the error signal are emitted.

3. Forward propagation (functional signal): Forward propagation (functional signal). Suppose a training example is represented by $(x(q), d(q))$, where $x(q)$ is the q-th input signal (vector) applied to the input layer of the network and d(q) is the vector that the network is expected to present at its output after training (desired response) for the input $x(q)$ (see Figure 3.6). Then, the linear combiners $v_m{}^{(t)}(q)$ and the functional signals $y_m{}^{(t)}(q)$ are obtained, in which the notations m and t represent the m-th neuron in the t-th layer of

the ANN. The equations 3.7 and 3.8 represent, respectively, the linear combiner and the functional signal.

$$v_m^{(t)}(q) = \sum_{l=0}^{L} w_{ml}^{(t)}(q) y_l^{(t-1)}(q) \tag{3.7}$$

$$y_m^{(t)} = \varphi_m \left(v_m \left(q_m \right) \right) \tag{3.8}$$

In these equations, L represents the total number of input signals coming from the previous layer $t-1$ in the m-th neuron of layer t, $y_l^{(t-1)}$ represents the functional signal obtained from the l-th output signal of the layer previous to t, $y_m^{(t)}$ is the output signal of the m-th neuron of layer t and $\phi(.)$ is the activation function of the network which can be the sigmoid function (Equation 3.3) or the hyperbolic tangent (Equation 3.7).

If neuron m is in the first hidden layer $(t=1)$, use Equation (3.9) in (3.7).

$$y_m^{(0)} = x_m(q) \tag{3.9}$$

When neuron m is in the output layer $(t=T)$, use Equation (3.10) to obtain the network's output signal.

$$z_m(q) = y_m^{(T)} \tag{3.10}$$

With the network output signal $z_m(q)$ and the desired response $d_m(q)$ for the m-th output neuron, calculate the error signal in (q), according to Equation 3.11.

$$e_m = d_m(q) - z_m(q) \tag{3.11}$$

4. Backpropagation (error signal): Calculate the local gradients of the network δ (Equation 3.12).

$$\delta_m^{(t)}(q) = \begin{bmatrix} e_m^{(T)}(q)\varphi_m' \left(v_m^{(T)}(q) \right) & \text{Neuron } m \text{ in the output layer } (T) \\ \\ \varphi_m' \left(v_m^{(t)}(q) \right) \sum_n \delta_n^{(t+1)}(q) w_{nm}^{(t+1)}(q) & \text{Neuron } m \text{ in the hidden layer } (t) \end{bmatrix}$$

$$\tag{3.12}$$

In the equation above, $\phi'_m(.)$ is the derivative of the activation function of the m-th neuron of layer t, for the case of the sigmoid function the derivative can be seen in Equation 3.5. With the values of the local gradients, modify the synaptic weights using Equation 3.13.

$$w_{ml}^{(t)}(q+1) = w_{ml}^{(t)}(q) + \alpha \left[w_{ml}^{(t)}(q) - w_{ml}^{(t)}(q-1) \right] + \eta \delta_m^{(t)}(q) y_l^{(t-1)}(q) \qquad (3.13)$$

In Equation 3.13, η and α are the learning rate and the momentum constant, respectively. Both the learning rate and the momentum constant are values chosen by the programmer and, preferably, should be between 0 and 1. These values may or may not vary during the training of the network, aiming to reduce the number of iterations and improve the result obtained by it.

5. Iteration: Presentation of the training data must be done several times, the number of iterations, that is, the number of times the training set must be presented, will depend on the stopping criterion chosen by the user.

CHAPTER 4

Modeling

Three architectures were developed, all three based on a multilayer perceptron network, trained by the Backpropagation algorithm. In Figure 4.1, the mental map of the architecture related to the neural network can be seen.

Figura 4.1: Mind map of the ANN architecture.
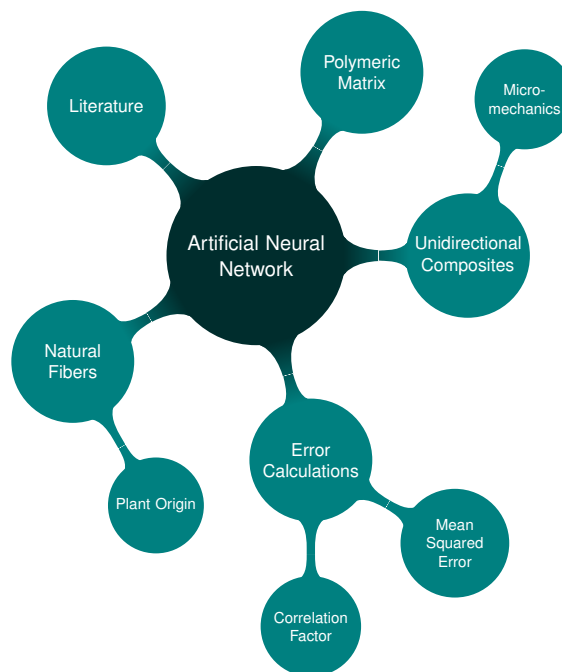
Source: Prepared by the author (2024).

Of the three architectures mentioned, two are composed exclusively of neural networks. One of these architectures has two inputs, while the other has three inputs. The third architecture is a hybrid approach, as illustrated in Figure 4.2, which uses a three-input ANN only to improve the results obtained by the equations of the model used.

Figura 4.2: Mind map of the Hybrid ANN architecture.
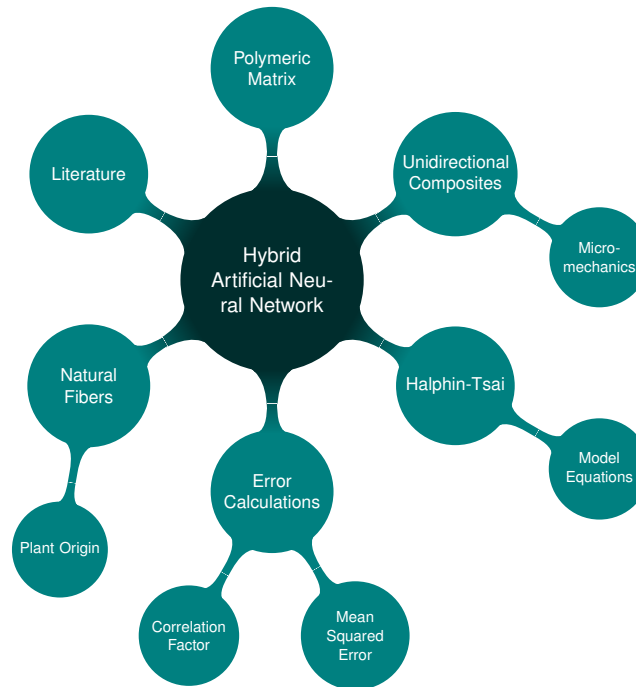
Source: Prepared by the author (2024).

Specifically, the Halpin-Tsai model was employed in the hybrid algorithm, and the "pure" Halpin-Tsai model was also used to serve as a comparison element for the previously proposed models.

The training of the three algorithms employed K-Fold cross-validation to evaluate performance during training. The data sets were divided into a training set (70% of the data set) and a test set (30% of the data set) in order to develop a network with good generalization capacity. All ANN architectures used two hidden layers with the number of neurons varying between 10 and 50 to verify which internal configuration would present the best results in this range. All neurons were biased and used the sigmoid activation function, except for the output neuron, which used the linear activation function. The training algorithm employed was backpropagation, based on the rule of moment (Haykin, 2001).

The two-input, three-input and hybrid models were trained for a maximum of 5000 epochs, using a learning rate of 0.005 and a momentum constant of 0.7 in all stages. It is important to highlight that both input neurons and output neurons had their data normalized to improve the learning of the ANN.

The correlation coefficient (r) and the MSE were analyzed. The study of these points, both for the ANN and for the Halpin-Tsai criterion, allowed the comparison between both and contributed to the validation of the ANN.

Below is Equation 4.1 from MSE, where E_{2real} is the "real" value of the transverse elastic modulus, coming from the experimental values, and E_{2rna} is the value calculated by ANN and the Halpin-Tsai equations. The term (n) is the amount of data used.

$$MSE = \frac{1}{2n} \sum \left(E_{\text{real}} - E_{\text{ann}}\right)^2 \tag{4.1}$$

4.1 Data Preprocessing

Data preprocessing is a crucial step in many data science and machine learning applications, including ANN modeling. It involves a series of techniques designed to prepare the raw data for modeling, ensuring that it is in a format suitable for use by machine learning algorithms (Paixão, Penido, Cury, & Mendes, 2022).

Data Obtained from the Literature

To determine the transverse modulus of elasticity, the following mechanical parameters of the unidirectional composites were required: fiber modulus of elasticity (E_f), matrix modulus of elasticity (E_m) and fiber volume fraction (V_f). The search for these data involved consulting scientific articles, books and technical reports (Agropecuária & GrandeIPB, 2009; Castro, 2013; de Castro & Grattapaglia, 2014; Ishizaki, Visconte, Furtado, Leite, & Leblanc, 2006; Kumaresan, Sathish, Karthi, et al., 2015; Lemos & Martins, 2014; Martin, Martins, Mattoso, & Silva, 2009; Martins, Iozzi, Martins, Mattoso, & Ferreira, 2004; Monteiro, Rodriguez, Lopes, & Sores, 2013; Pinto, A Júnior, Carvalho, et al., 2005; Prasad, Gowda, & Velmurugan, 2017; S. O. Silva, 2021; T. L. S. Silva, de Oliveira Filho, & do Nascimento Silva., 2024).

In the ANN training process, data from 74 unidirectional composites were initially collected to form the initial data set. However, to increase the representativeness of the data set, an interpolation was performed, expanding the number of composites to 300. With this new expanded set, the distribution between training and testing data now has 210 composites intended for training and 90 for testing.

These composites covered a variety of materials for the fiber and matrix, as well as different fiber percentages, ranging from 20% to 70%. It is important to emphasize that, for the determination of the transverse modulus of elasticity, only unidirectional sheets were used in the entire data set.

The fibers used in the manufacture of the unidirectional sheets were made of various types of materials, including sisal fiber (*agave sisalana*), jute, and coconut. The matrices evaluated were: polyester, epoxide, polypropylene, and polyurethane.

Tables 4.1, 4.2, and 4.3 present, respectively, the values of the transverse elasticity moduli of the fiber, the matrix, and the unidirectional composites used during the study.

Tabela 4.1: Values collected from the literature for the transverse modulus of elasticity for fibers.

Fibers	Fiber Modulus (GPa)
Sisal	$3.62 - 9.17$
Jute	$10.19 - 11.04$
Coconut	$1.54 - 2.50$

Source: Prepared by the author (2024).

Tabela 4.2: Values collected from the literature for the transverse modulus of elasticity for matrix.

Matrix	Matrix Modulus (GPa)
Polyester	$2.06 - 4.41$
Epoxy	$2.3 - 4.6$
Polypropylene	$1.14 - 1.55$
Polyurethane	$1.1 - 3.6$

Source: Prepared by the author (2024).

Tabela 4.3: Values of the transverse modulus of elasticity for unidirectional composites.

Composite	Transverse Modulus (GPa)
Sisal/Epoxy	$6.33 - 13.44$
Sisal/Polyester	$6.11 - 13.21$
Sisal/Polyurethane	$1.78 - 6.14$
Jute/Epoxy	$6.53 - 14.90$
Jute/Polyester	$6.30 - 14.71$
Jute/Polypropylene	$2.12 - 7.30$
Coconut/Epoxy	$4.53 - 5.56$
Coconut/Polyester	$4.65 - 5.41$
Coconut/Polyurethane	$1.31 - 2.56$

Source: Prepared by the author (2024).

Data Interpolation

A fundamental aspect of the data preparation process for analysis was the application of linear interpolation. Initially, the dataset consisted of 74 unidirectional composites. Recognizing the need to increase the representativeness of the dataset, it was decided to perform linear interpolation. This technique allowed expanding the dataset to a total of 300 composites (S. Silva et al., 2020).

This expansion was essential to ensure a more comprehensive and representative distribution of data, which is essential for training neural network models (Dantas et al., 2020).

Data Normalization

Normalization is a fundamental technique in many areas of data science and machine learning, and is essential for preparing data before applying training algorithms or statistical analysis (Lima, 2021).

Among the various normalization approaches, Min-Max normalization stands out as one of the simplest and most widely used, allowing a more consistent comparison between different data sets or variables. It is important to highlight that, since the volumetric fraction varies from 0 to 1, there was no need to normalize this input parameter (Lopes, 2024).

The original value E_2 is adjusted to E_{2nor} so that it is in the scale between E_{2min} and E_{2max}.

$$E_{2\text{nor}} = \frac{E_2 - E_{2\text{min}}}{E_{2\text{max}} - E_{2\text{min}}} \tag{4.2}$$

where:

$E_{2\text{nor}}$ is the normalized value,

E_2 is the original value of the transverse modulus of elasticity,

$E_{2\text{min}}$ is the minimum value in the data set,

$E_{2\text{max}}$ is the maximum value in the data set.

The original value E_f is adjusted to $E_{f\,nor}$ so that it is on the scale between $E_{f\,min}$ and $E_{f\,max}$.

$$E_{f\,\text{nor}} = \frac{E_f - E_{f\,\text{min}}}{E_{f\,\text{max}} - E_{f\,\text{min}}} \tag{4.3}$$

where:

$E_{f\,\text{nor}}$ is the normalized value,

E_f is the original value of the fiber modulus of elasticity,

$E_{f\,\text{min}}$ is the minimum value in the data set,

$E_{f\,\text{max}}$ is the maximum value in the data set.

The original value E_m is adjusted to E_{mnor} so that it is on the scale between E_{mmin} and E_{mmax}.

$$E_{m\text{nor}} = \frac{E_m - E_{m\text{min}}}{E_{m\text{max}} - E_{m\text{min}}}$$

(4.4)

where:

$E_{m\text{nor}}$ is the normalized value,

E_m is the original value of the matrix modulus of elasticity,

$E_{m\text{min}}$ is the minimum value in the data set,

$E_{m\text{max}}$ is the maximum value in the data set.

Resampling methods

Resampling methods are indispensable tools in modern statistics. The techniques involve partitioning the training data and refitting the competing models for each subsample in order to obtain additional information about the model fit, something that would not be possible with the full data (Ferreira, 2018).

Figura 4.3: Erro de predição por complexidade do modelo.
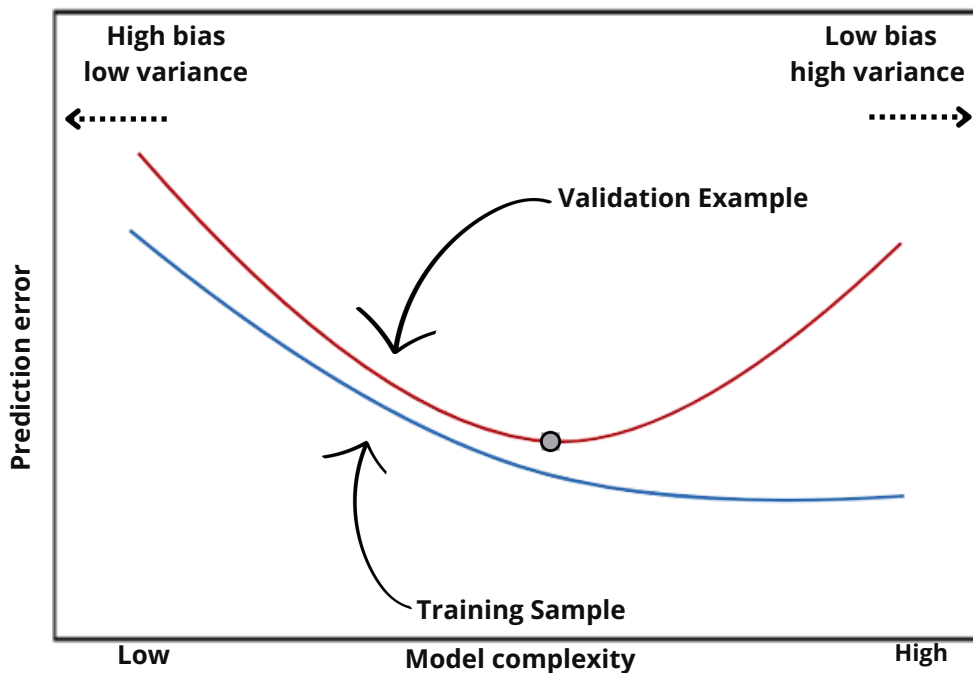
Fonte: Adaptado de Ferreira (2018).

For example, through resampling methods, we can estimate the test error associated with a given model and perform model selection with the appropriate level of flexibility (Ferreira, 2018).

This translates into training the algorithm with a training sample represented by the blue curve in Figure 4.3 and evaluating the goodness of fit with a validation sample, indicated by the red curve. It is important to note that using very simple algorithms will result in a high prediction error in the training sample, represented by the blue curve, while increasing model complexity tends to reduce this training error.

However, this apparent improvement is accompanied by a decrease in generalization capacity, that is, the model's performance when dealing with new examples, such as the validation sample, may be unsatisfactory.

Given this issue, the challenge lies in finding a balance between a simple model, which may be underfit, and a complex model, which may be overfit, so that error is minimized when new data is introduced.

K-Fold Cross-Validation

Separating the data into only two disjoint parts can yield divergent results, depending on the information contained in each set, especially when the data is scarce. The k-fold cross-validation approach minimizes these problems (Leal, 2019).

The method consists of dividing the data into K equal parts, adjusting the model using K-1 parts, and the remaining portion is destined for validation. This process is repeated K times, at each moment a different partition will be the validation; then, the results are combined, obtaining the average of the errors obtained (Cunha, 2019).

Definition:

- Let K parts denoted by $C_1, C_2, \ldots, C_K$, where C_k represents the index of the k-th part.

- Assume that we have n_k observations in partition k (if n is a multiple of K, then $n_k = \dfrac{n}{K}$).

- Calculate:

$$CV_{(K)} = \sum_{k=1}^{K} \frac{n_k}{n} MSE_k, \qquad (4.5)$$

where $MSE_k = \dfrac{\sum_{i \in C_k} (y_i - \hat{y}_i)^2}{n_k}$, and $\hat{y}_i$ is the adjusted value of observation i, obtained from the data with the k-th part removed. The k-fold cross-validation approach is represented in Figure 4.4.

Figura 4.4: Validação cruzada por k-fold.

$$\bar{E} = \frac{1}{k} \sum_{i=1}^{k} E_i \tag{4.6}$$

where:

$\bar{E}$ represents the average metric across all folds.

k is the total number of folds in k-fold cross-validation.

E_i is the performance metric in the i-th fold.

This Equation 4.6 computes the average of the performance metric (E) over all folds in a k-fold cross-validation, where E_i is the performance metric on the i -th fold. The sum is taken over all folds from 1 to k, and the result is then divided by the total number of folds k to obtain the average.

4.2 Two-Input ANN Model

The ANN architecture represented in Figure 4.5 is provided by two input neurons and one output neuron.

Figura 4.5: Neural network architecture with two inputs.
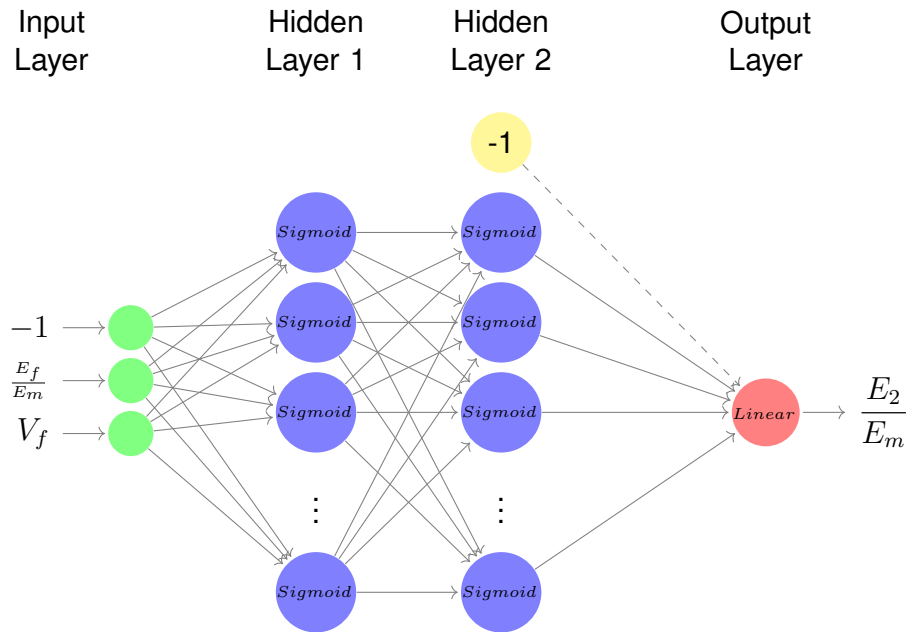
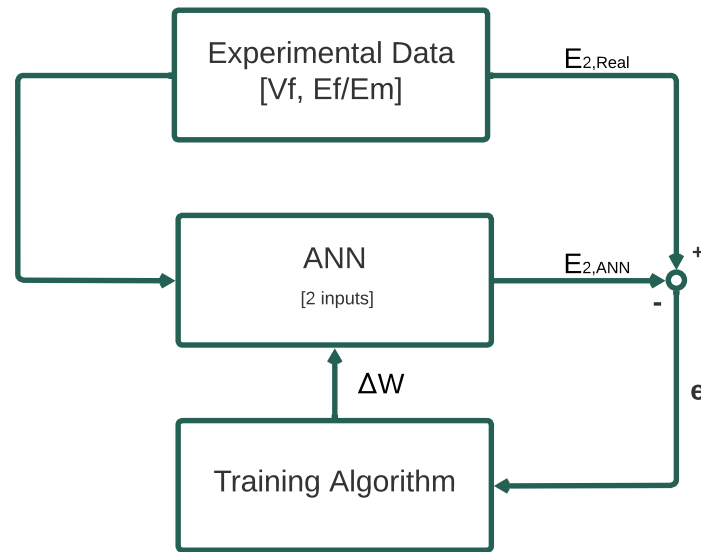**Source:** Adapted from Oliveira (2018).

Therefore, an input neuron that represents the ratio of the fiber's modulus of elasticity to the matrix's modulus of elasticity, an input neuron that represents the fiber volume, and an output neuron represented by the ratio of the transverse modulus of elasticity to the matrix's modulus of elasticity.

Equation 4.7 aims to model with the ANN, where, $\frac{E_f}{E_m}$ is the ratio of the fiber's modulus of elasticity to the matrix's modulus of elasticity, $\frac{E_2}{E_m}$ represents the ratio of the transverse modulus of elasticity to the matrix's modulus of elasticity, and V_f is the fiber volume.

$$\frac{E_2}{E_m} = \mathrm{f}\left(\frac{E_f}{E_m}, V_f\right) \tag{4.7}$$

In this specific type of architecture, its main function is to simplify the data used, reducing the number of synaptic weights in the network. In Figure 4.6, the training architecture of the ANN with two inputs can be seen.

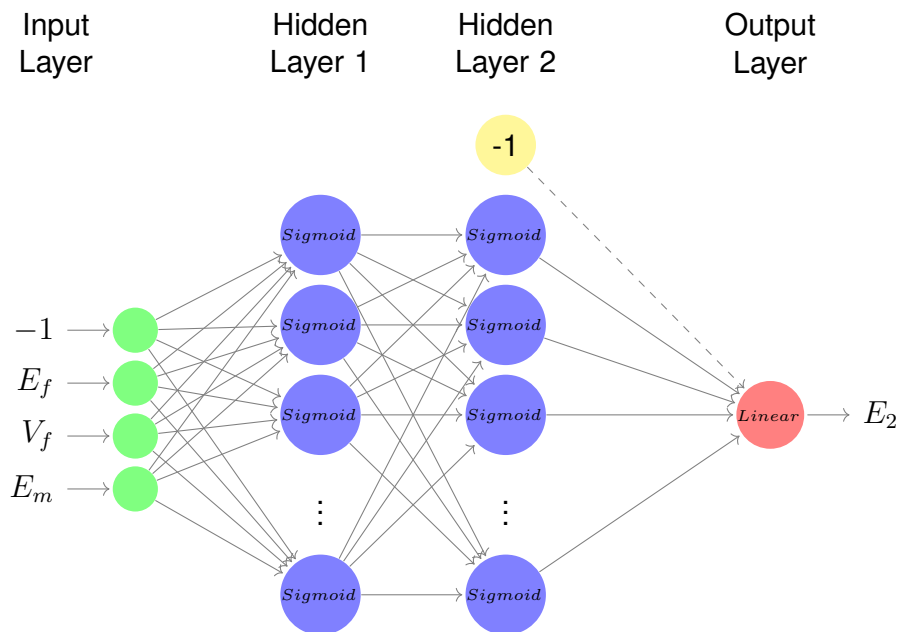Figura 4.6: Training architecture for ANN with two inputs.

Source: Adapted from E. C. B. Câmara (2012).

4.3 Three-Input ANN Model

The ANN architecture represented in Figure 4.7 consists of three input neurons and one output neuron.

Figura 4.7: Neural network architecture with three inputs.

**Source:** Adapted from Oliveira (2018).

Therefore, an input neuron representing the fiber's modulus of elasticity, an input neuron representing the fiber volume, an input neuron representing the matrix's modulus of elasticity, and an output neuron representing the transverse modulus of elasticity.

Equation 4.8 has the function that aims to model the three-input architecture. Therefore, E_2 is the transverse modulus of elasticity, E_f is the fiber's modulus of elasticity, E_m is the matrix's modulus of elasticity, and V_f is the fiber volume.

$$E_2 = \mathrm{f}\left(E_f, E_m, V_f\right) \tag{4.8}$$

In Figure 4.8, the training architecture of this ANN is shown, changing the data types that will serve as comparison for the operation of the backpropagation algorithm, represented by ΔW the update of the synaptic weights, coming from the training algorithm.

Figura 4.8: Arquitetura de treinamento para RNA três entradas.
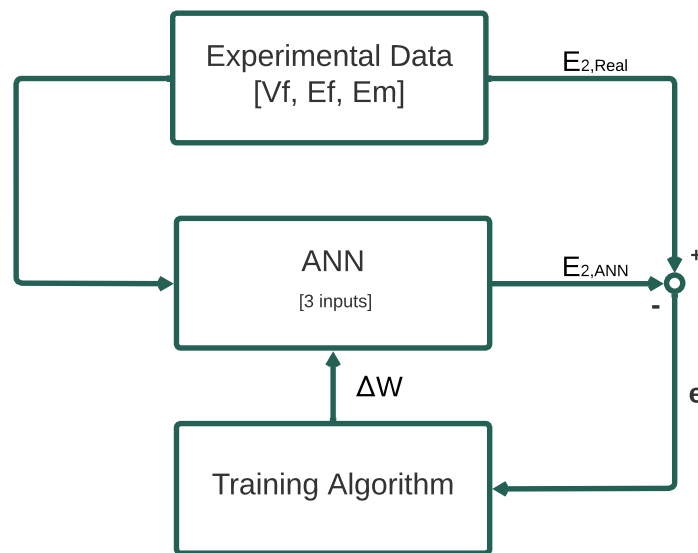
Fonte: Adaptado de E. C. B. Câmara (2012).

4.4 Three-Input Hybrid RNA Model

The hybrid model has a structure formed by a ANN and a semi-empirical calculation model, using the Halpin-Tsai model. Its application will have the function of approximating the analytical model of the result of (E_{2real}) to the values obtained experimentally, taken from the literature.

For this example, the output of ANN is the error (ed), which is given by the difference between the experimentally obtained transverse elastic moduli (E_{2real}) values and the transverse elastic moduli values obtained from the Halpin-Tsai equations ($E_{2estimado}$).

$$e_d = E_{2\,\text{real}} - E_{2\,\text{estimado}} \tag{4.9}$$

In Figure 4.9, the value of ΔW represents the update of the synaptic weights, coming from the training algorithm. There is an analytical approximation to obtain the value of E_2, however, in order to improve the results, a ANN is used.

Figura 4.9: Training architecture and flowchart of the three-input neural network with Halphin-Tsai.
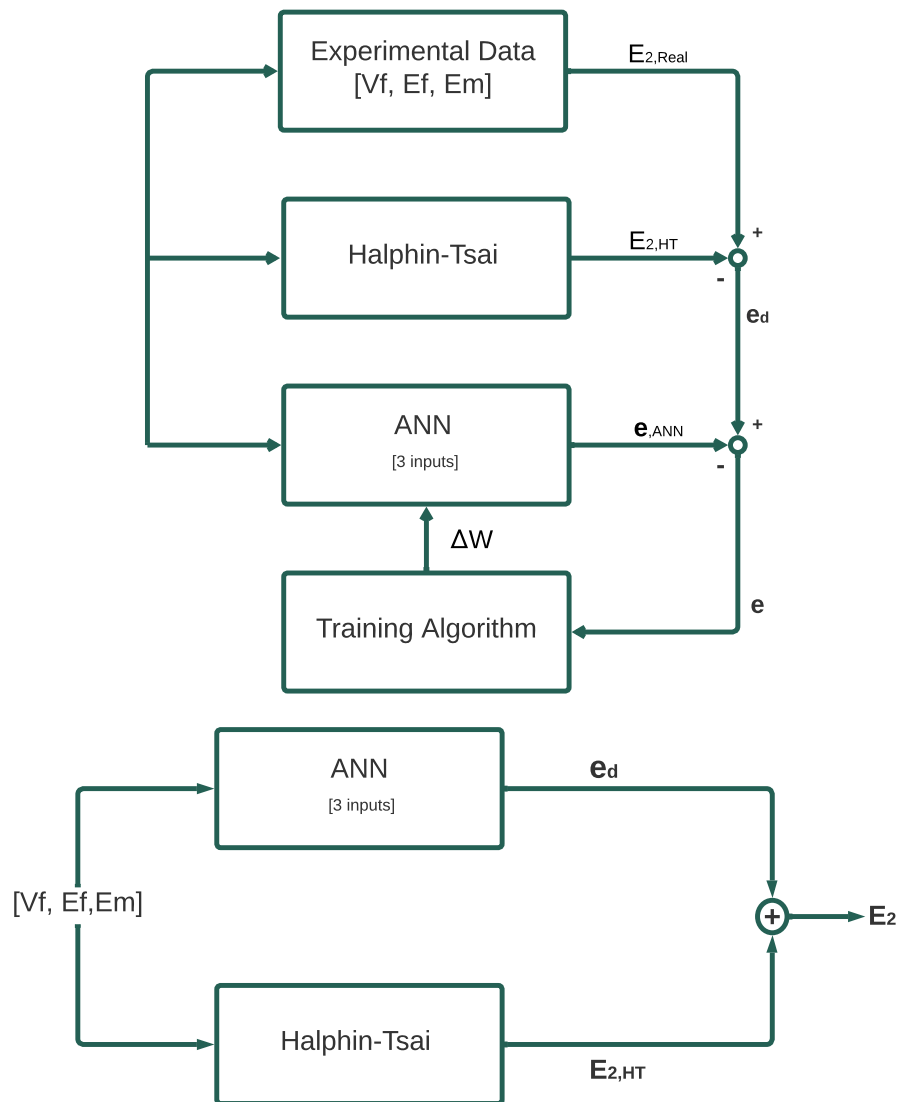
**Source:** Adapted from E. C. B. Câmara (2012).

Results

In this section, the main results of the Artificial Neural Network (ANN) training for the analysis of the mechanical property E_2 will be shown, together with its proposed two- and three-input models, in addition to the hybrid model. A comparison will also be made to validate the ANN related to the transverse modulus of elasticity (E_2), and the theoretical model (Halpin-Tsai). To provide a starting point for the analysis, the results obtained by the Halpin-Tsai model are compared to the experimental data. The MSE obtained between the experimental data and the Halpin-Tsai model was 0.006574, while the correlation coefficient was 0.9131.

5.1 Two-Input ANN

Using cross-validation, the MSE of the ANN was initially evaluated in relation to the network's training epochs. In the case of a two-input architecture, it was found that, despite the lower MSE values obtained for the test data set, the values for the training data set remained high, as illustrated in Figure 5.1, reaching approximately 0.006986, higher than the Halpin-Tsai model, which reached 0.006574. Furthermore, it is observed that at the beginning of training there is no significant reduction in the MSE of the training set, which will probably result in a ANN unable to generalize and model the data satisfactorily.

In Figure 5.2, a comparative analysis was performed focusing on the E_2 values generated by ANN. The training and test data were analyzed in a value graph, where it is noticeable that the closer these values are to the red line, the greater the linearity between the ANN and experimental values. The values were well distributed for low values, while for higher values, ANN found values lower than the experimental ones. In this model, it is observed that the test data had values far from the comparative line.

Figura 5.1: Mean Squared Error (MSE) Analysis by the Number of Training Epochs for the Two-Input Neural Network.
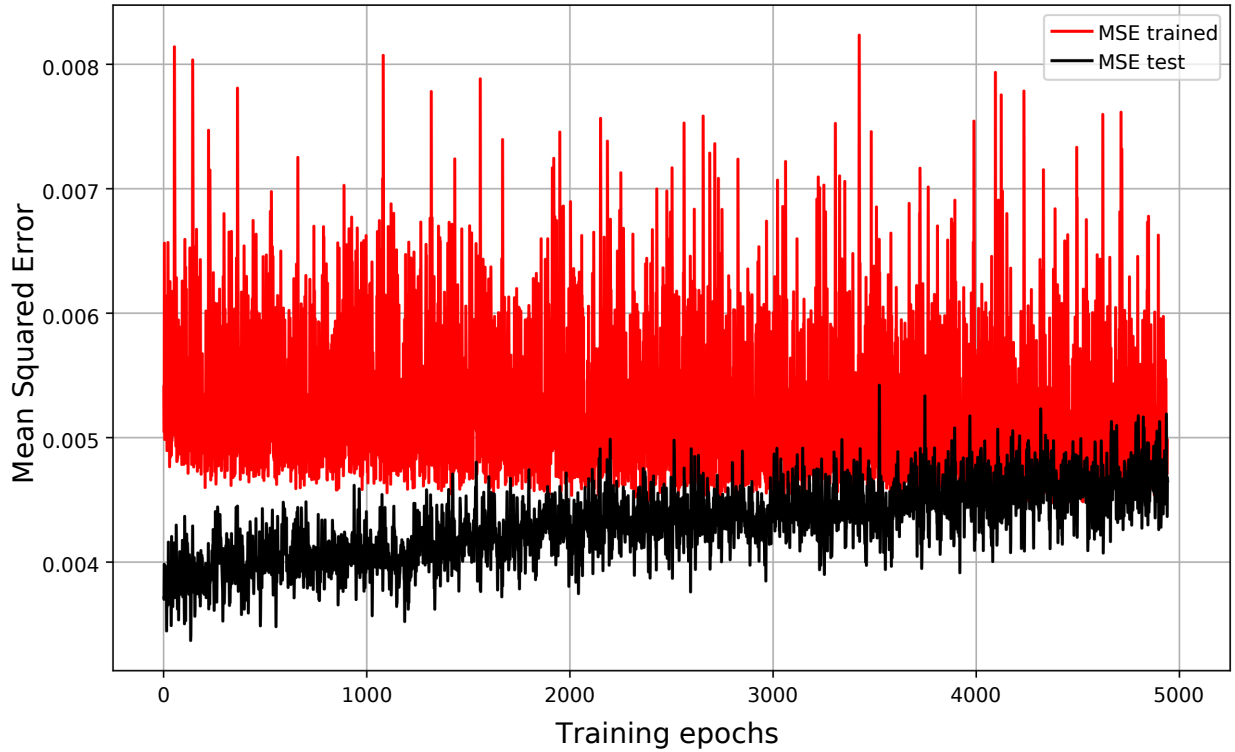
Source: Prepared by the author (2024).

Figura 5.2: Comparative Graph of the Two-Input Neural Network.
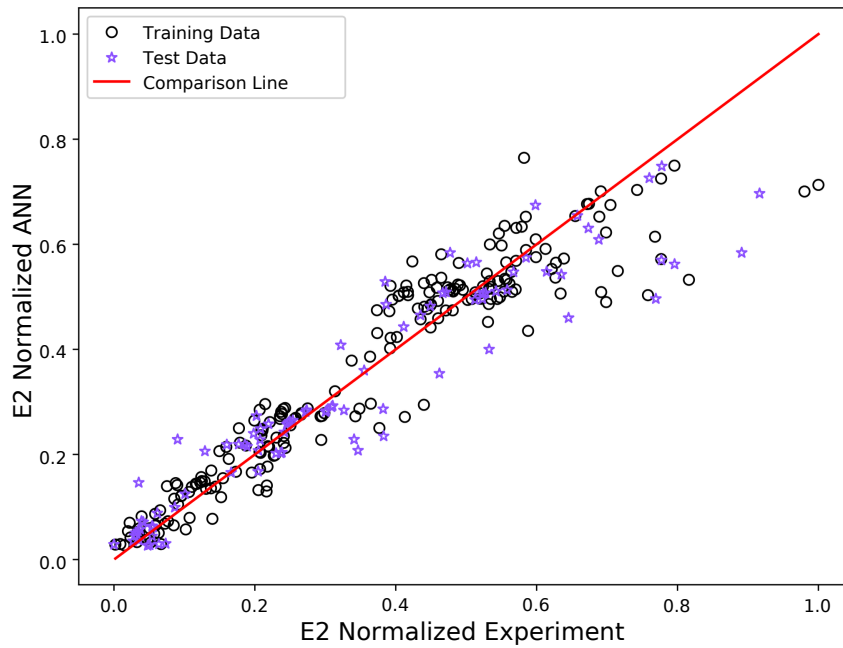
Source: Prepared by the author (2024).

5.2   Three-Input ANN

As done in the previous architecture, cross-validation was again used as the stopping criterion for this ANN. In other words, a test set was used to choose the synaptic weights of the ANN. Analyzing the mean square error curve as a function of the number of training epochs for the best result obtained, which was with 48 neurons in the hidden layer, as shown in Figure 5.3, it can be seen that there is a tracking of the two curves in the same order of magnitude. This behavior did not occur in the two-input ANN, where a significant difference was observed between the data. This fact may serve as an indication that the three-input ANN is managing to generalize the micromechanical behavior better than the two-input ANN.

In Figure 5.4, a comparative analysis similar to that done with the two-input ANN was performed, focusing on the E_2 values generated by the ANN. The values showed a good distribution for the low values, while, for higher values, there was an improvement in relation to the two-input ANN, especially in the lower values of the experimental data. In this model, it is observed that the test data showed an improvement in comparison with the two-input ANN, considering the comparative line.

Figura 5.3: Mean Squared Error (MSE) Analysis by the Number of Training Epochs for the Three-Input Neural Network.
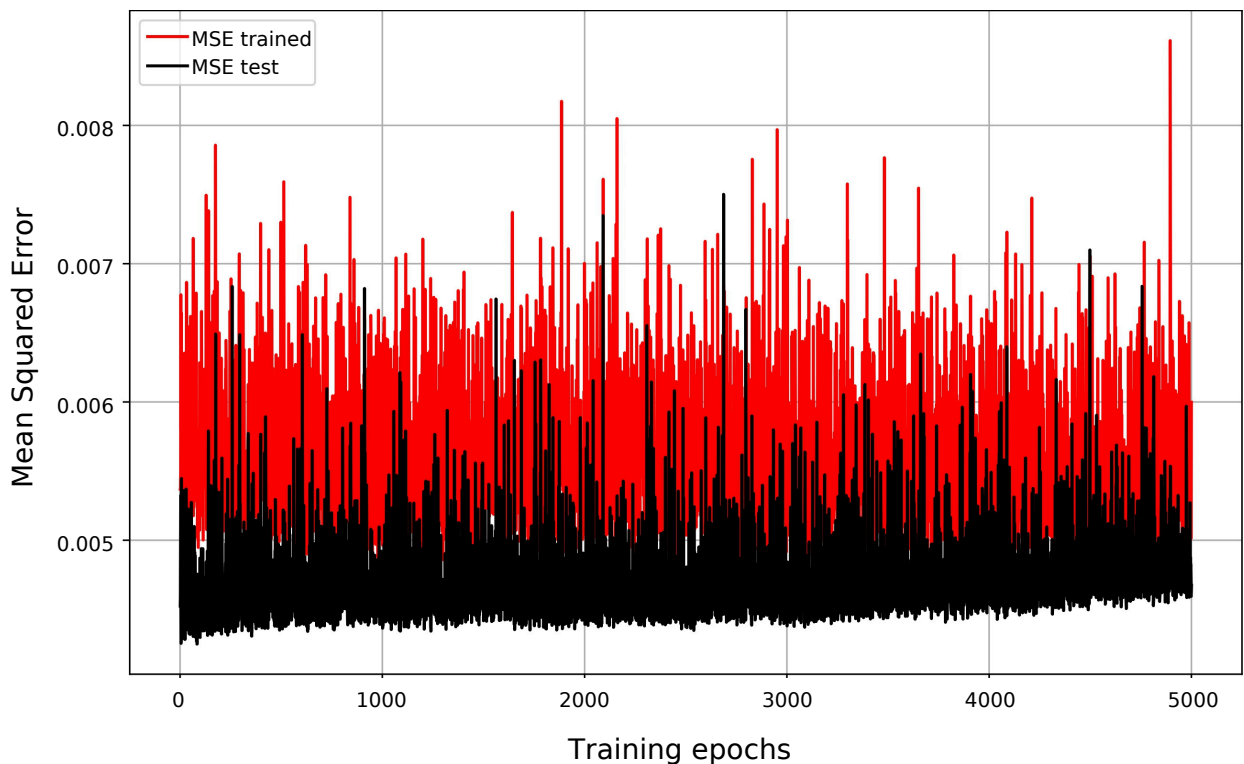
Source: Prepared by the author (2024).

Figura 5.4: Comparative Graph of the Three-Input Neural Network.
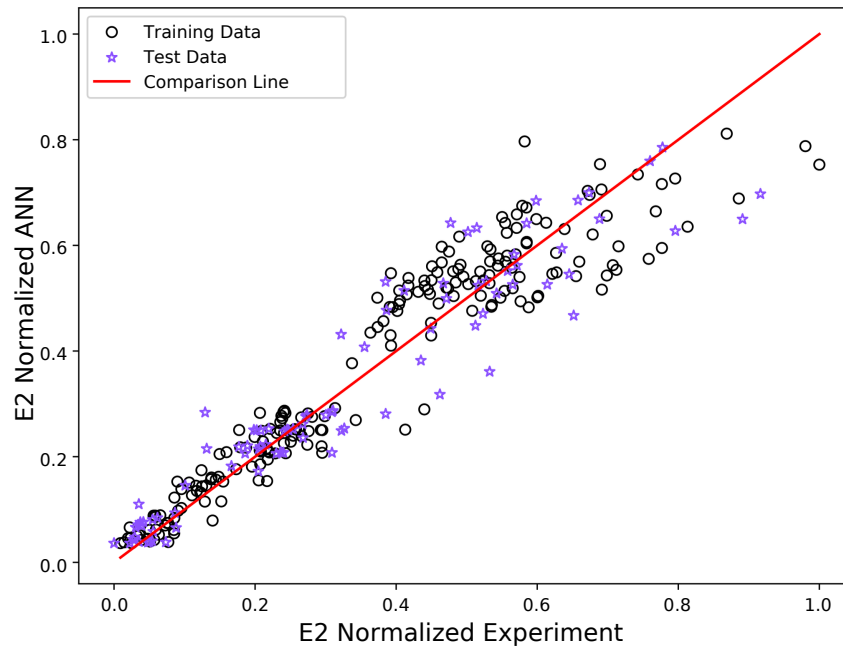
Source: Prepared by the author (2024).

5.3 Three-Input ANN Hybrid Model.

The hybrid modeling used here combines a theoretical Halpin-Tsai model with a ANN to adequately adjust the experimental data. In any case, as in the two previous architectures, cross-validation was used as a stopping criterion, seeking to obtain the most appropriate response to the experimental data.

Thinking in this way, the architecture that presented the best results has 24 neurons in the hidden layer. As can be seen in Figure 5.5, which shows the mean square error values for the training and test sets, this result was observed in the three-input ANN, which also presented satisfactory results and was not observed in the two-input ANN, whose results proved to be unreliable. With this result, it can be seen that the mixed model may also have the ability to generalize the micromechanical behavior of unidirectional blades.

The Hybrid model is based on the values of the semi-empirical Halpin-Tsai equations to, together with a ANN, perform an adjustment on these equations in order to bring their results closer to the experimental values. In this model, a greater proximity of the values of the mixed ANN to the real values is observed, mainly in the training data, when compared to the other models. In Figure 5.6, it is also observed that the values were closer to the comparative line.

Figura 5.5: Mean Squared Error (MSE) Analysis by the Number of Training Epochs for the Hybrid Model Neural Network.
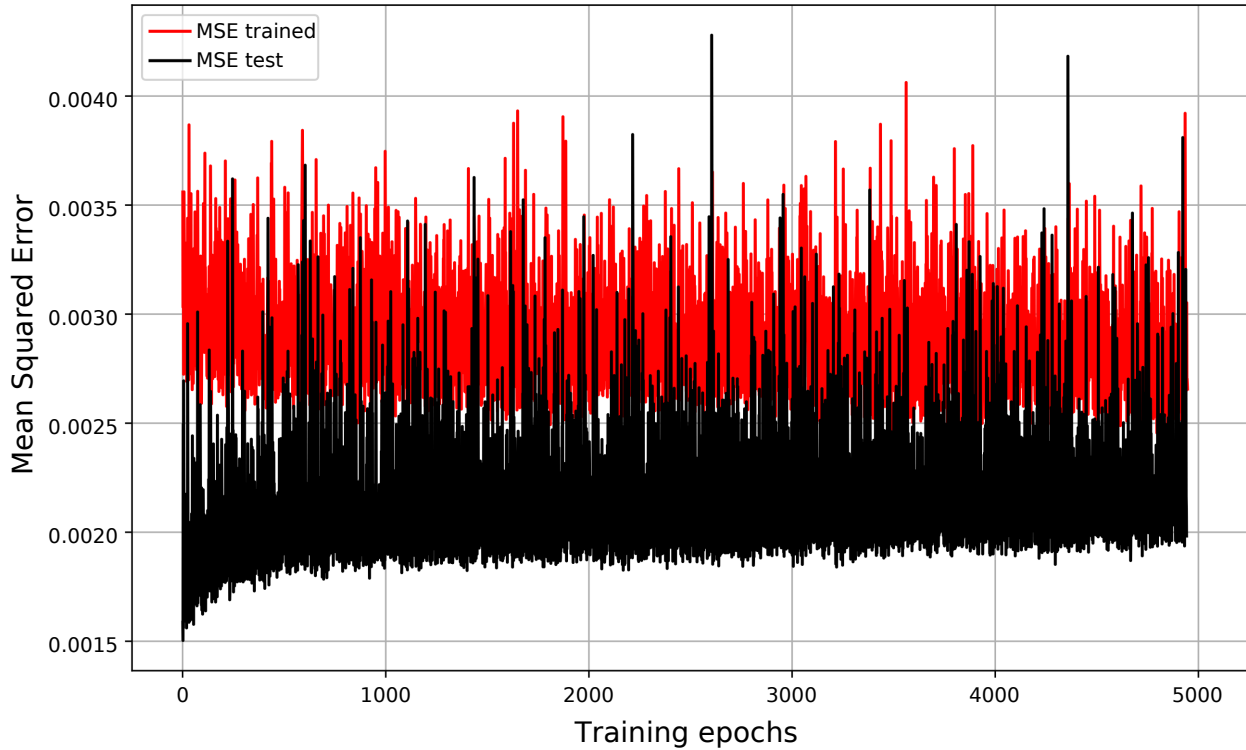
Source: Prepared by the author (2024).

Figura 5.6: Comparative Graph of the Hybrid Model Neural Network.
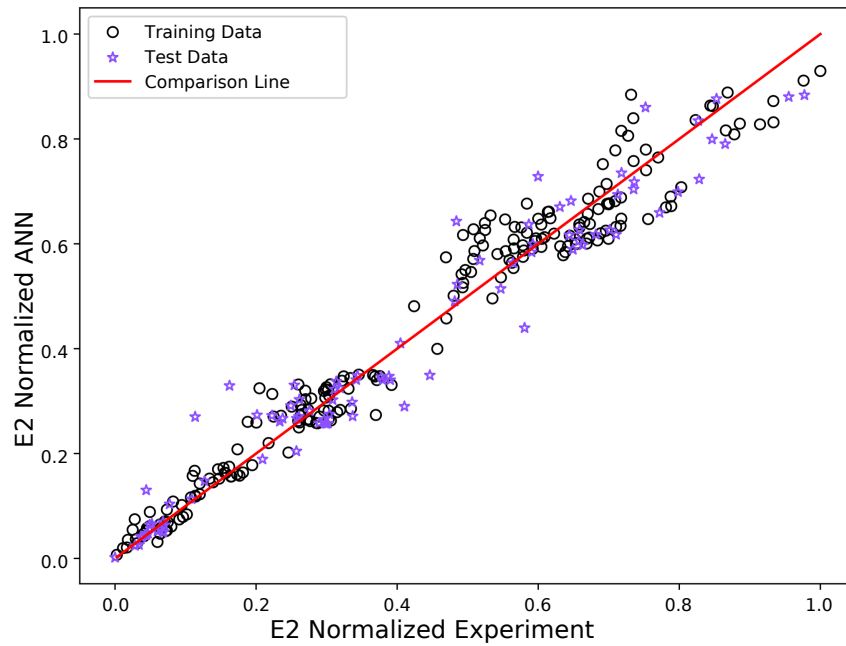
Source: Prepared by the author (2024).

5.4 Comparative Analysis

Using table 5.1, it is possible to perform a comparative analysis of all the models described in the previous items. The three-input ANN model and the mixed model achieved the best results, while the two-input ANN model obtained unsatisfactory results and worse than the Halpin-Tsai model. It can also be observed that the MSE of the mixed model is lower than that of all the other models, with a value approximately 36.6% lower than that of the three-input model. The difference between these results is best exemplified in Figure 5.7, which shows a bar graph with the mean square error values. It should be noted that the training of these models was done under the same conditions and these values were taken from the training sessions that obtained the best results in relation to the number of neurons and training epochs.

Tabela 5.1: Comparison of the ANN models with the Halpin-Tsai model.

Model	MSE	r	Training Epochs	Number of Neurons (Hidden Layer)
ANN with two inputs	0.006986	0.9025	5000	12
ANN with three inputs	0.006172	0.9358	5000	48
Hybrid ANN with three inputs	0.003913	0.9582	5000	24
Halpin-Tsai	0.006574	0.9131	- - - -	- - - -

Source: Prepared by the author (2024).

Figura 5.7: Bar Chart for MSE Analysis
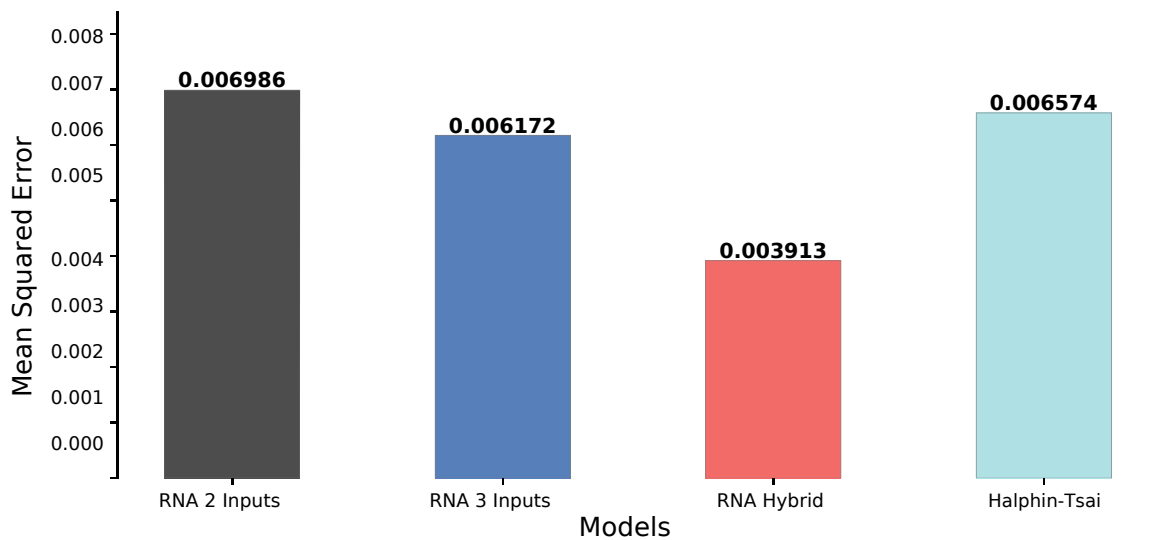
Source: Prepared by the author (2024).

Conclusion

After analyzing the results obtained, we conclude that the use of a hybrid model (RNA/Halpin-Tsai) produces results that enable its use in the field of composite materials. This model has proven useful in the development and testing of transverse elasticity moduli of new composites, since the parameters used provided superior results to those obtained by the Halpin-Tsai models and other ANN alone.

The ANN with two inputs did not meet expectations, failing to adequately model the transverse elasticity modulus and, therefore, is not reliable for use. This unsatisfactory performance can be attributed to the simplicity of the architecture, which does not correspond to the desired behavior. The MSE obtained for the test data set of the two-input ANN was approximately 0.006986, higher than the Halpin-Tsai model, which achieved 0.006574, indicating inferior performance. Furthermore, at the beginning of the training there was no significant reduction in the MSE of the training set, which probably results in a ANN incapable of generalizing and modeling the data satisfactorily.

The ANN with three inputs presented more satisfactory results in the qualitative and quantitative analyses compared to the Halpin-Tsai model. Analyzing the mean square error curve as a function of the number of training epochs, it was observed that there was a follow-up of the two curves in the same order of magnitude, suggesting a better generalization of the micromechanical behavior.

The three-input ANN achieved significantly better results than the two-input ANN, with a better distribution of the generated E_2 values and a greater approximation of the experimental values.

In the comparative analysis of the E_2 values generated by the three-input ANN, the values showed a good distribution for the low values and, for higher values, there was an improvement in relation to the two-input ANN, especially in the lower values of the experimental data.

A crucial difference between these two types of modeling is that the hybrid model generalizes better, since it is based on both the ANN and the data from the Halpin Tsai model. The combination of the values from the semi-empirical Halpin-Tsai equations with the ANN allowed a closer approximation of the experimental results, especially in the training data. The MSE of the hybrid model was approximately 36.6% lower than that of the three-input ANN, demonstrating its superiority.

In the comparative analysis of the E_2 values generated by the hybrid model, a greater proximity to the real values is observed, especially in the training data, when compared to the other models. In contrast, the ANN with three inputs, because it depends only on the training of the algorithm, requires a significant amount of data to obtain and present good results.

Therefore, the adoption of the hybrid model is recommended for the analysis of the transverse modulus of elasticity in composite materials, offering a more robust and accurate approach, especially in contexts where the available data are not sufficiently extensive.

Bibliographic References

Affdl, J. H., & Kardos, J. (1976). The halpin-tsai equations: a review. *Polymer Engineering & Science*, *16*(5), 344–352.

Agropecuária, E. I., & GrandeIPB, C. (2009). Caracterização química e estrutural de fibra de sisal da variedade agave sisalana.

Araújo, R. K. F. (2019). Estudo térmico e mecânico de placas cimentícias, simulando uma estrutura de wood frame com uso de vermiculita expandida e fibra de sisal. *Universidade Federal Rural do Semi-Árido*.

Bank, L. C. (2006). *Composites for construction: structural design with frp materials*. John Wiley & Sons.

Callister, W. D., & Rethwisch, D. G. (2020). *Fundamentals of materials science and engineering: an integrated approach*. John Wiley & Sons.

Câmara, E. C. B. (2012). *Previsão do módulo de elasticidade transversal de compósitos unidirecionais através de redes neurais mistas* (Unpublished master's thesis). Universidade Federal do Rio Grande do Norte.

Câmara, M. (2014). Anatomia e fisiologia humana. *Instituto de Formação–Cursos Técnicos Profissionalizantes*.

Castro, B. F. M. (2013). *Estudo e caracterização mecânica de compósitos reforçados com fibras naturais* (Unpublished doctoral dissertation). Instituto Politécnico do Porto. Instituto Superior de Engenharia do Porto.

Cavalcante, M. d. S. (2018). Materiais híbridos orgânicos-inorgânicos: argilominerais, óxidos e polímeros.

Costa, G. Y. S. C. M., et al. (2021). Aplicação de aprendizado de máquina na predição do rendimento da fermentação de alginase.

Cunha, J. P. Z. (2019). *Um estudo comparativo das técnicas de validação cruzada aplicadas a modelos mistos* (Unpublished doctoral dissertation). Universidade de São Paulo.

Dantas, D., Calegario, N., Acerbi, F. W., Carvalho, S. d. P. C., Isaac, M. A., & Melo, E. d. A. (2020). Multilevel nonlinear mixed-effects model and machine learning for predicting the volume of eucalyptus spp. trees. *Cerne*, *26*(1), 48–57.

de Castro, L. A. B., & Grattapaglia, D. (2014). The 5th congress of the brazilian biotechnology society (sbbiotec): Meeting abstracts. In *Bmc proceedings* (Vol. 8, pp. I1–P264).

de Mendonça, P. d. T. R. (2005). *Materiais compostos e estruturas-sanduíche: projeto e análise*. Manole.

Diniz, C. A., da Cunha Júnior, S. S., Júnior, A. C. A., Gomes, G. F., Bicalho, R., & Campos, R. B. (2016). Otimização estrutural de elementos em compósitos usando redes neurais artificiais. *Revista Interdisciplinar de Pesquisa em Engenharia*, *2*(10), 51–60.

Eichhorn, S., Hearle, J. W., Jaffe, M., & Kikutani, T. (2009). Handbook of textile fibre structure: Volume 2: Natural, regenerated, inorganic and specialist fibres.

Fahlman, S. E., et al. (1988). *An empirical study of learning speed in back-propagation networks*. Carnegie Mellon University, Computer Science Department Pittsburgh, PA, USA.

Faruk, O., Bledzki, A. K., Fink, H.-P., & Sain, M. (2012). Biocomposites reinforced with natural fibers: 2000–2010. *Progress in polymer science*, *37*(11), 1552–1596.

Felipe, R. N. B. (2012). Efeitos da radiação uv, temperatura e vapor aquecido nos compósitos poliméricos: monitoramento, instabilidade estrutural e fratura.

Ferreira, E. V. (2018). Métodos de reamostragem. *Material de apoio a disciplina de Machine Learning para Cientista de Dados, lecionada na LEG/UFPR*, *16*, 17.

Freire Jr, R. C. S., & Aquino, E. M. F. d. (2005). Fatigue damage mechanism and failure prevention in fiberglass reinforced plastic. *Materials Research*, *8*, 45–49.

Géron, A. (2019). *Mãos à obra: Aprendizado de máquina com scikit-learn & tensorflow*. Alta Books.

Godoy, A. P. (2019). Utilização de líquidos iônicos na esfoliação em fase líquida do grafite e aplicação na formação de nanocompósitos condutores de polímero-grafeno para impressão 3d.

Goleman, D. (2017). *Inteligência ecológica: o impacto do que consumimos e as mudanças que podem melhorar o planeta*. Elsevier Brasil.

Halpin, J. C., & Tsai, S. (1969). Effects of environmental factors on composite materials.

Haykin, S. (2001). *Redes neurais: princípios e prática*. Bookman Editora.

Ishizaki, M. H., Visconte, L. L., Furtado, C. R., Leite, M. C., & Leblanc, J. L. (2006). Caracterização mecânica e morfológica de compósitos de polipropileno e fibras de coco verde: influência do teor de fibra e das condições de mistura. *Polímeros*, *16*, 182–186.

Júnior, R. C. S. F., Neto, A. D. D., & de Aquino, E. M. F. (2005). Building of constant life diagrams of fatigue using artificialneural networks. *International Journal of Fatigue*, *27*(7), 746–751.

Kaw, A. K. (2005). *Mechanics of composite materials*. CRC press.

Kumaresan, M., Sathish, S., Karthi, N., et al. (2015). Effect of fiber orientation on mechanical

properties of sisal fiber reinforced epoxy composites. *Journal of Applied Science and Engineering*, *18*(3), 289–294.

Leal, M. d. O. C. D. (2019). *Estimativa do sexo em amostras brasileiras com validação cruzada em populações de diferentes regiões* (Unpublished doctoral dissertation). [sn].

Leão, J. F. A. (2018). Critérios de falha e modelos analíticos para análise local em dutos flexíveis com armaduras de tração em material compósito.

Leão, M. A. (2013). Compósitos poliméricos a base de fibras de licuri: efeitos da hibridização e do envelhecimento ambiental acelerado.

Lemos, A. L. d., & Martins, R. M. d. (2014). Desenvolvimento e caracterização de compósitos poliméricos à base de poli (ácido lático) e fibras naturais. *Polímeros*, *24*, 190–197.

Líbano, E. V. D. G., da Costa Pereira, P. S., Bastos, D. C., de Souza Coelho, K. V., et al. (2020). Estudo da influência do teor de fibras e de compatibilizante na obtenção de compósitos de polietileno de alta densidade pós-consumo (peadpc) com fibras de bagaço de cana-de-açúcar (bca). *Cadernos UniFOA*, *15*(43).

Lima, M. P. S. d. (2021). *Avaliação de estratégias de decisão de mobilidade madm orientados para a qualidade em cenário de redes 5g* (Unpublished master's thesis). Universidade Federal do Rio Grande do Norte.

Lopes, V. H. S. (2024). Análise comparativa do pré-processamento de dados na classificação de sementes.

Lorandi, N. P., Cioffi, M. O. H., & Ornaghi Jr, H. (2016). Análise dinâmico-mecânica de materiais compósitos poliméricos. *Sci Cum Ind*, *4*(13), 48–60.

Martin, A. R., Martins, M. A., Mattoso, L. H., & Silva, O. R. (2009). Caracterização química e estrutural de fibra de sisal da variedade agave sisalana. *Polímeros*, *19*, 40–46.

Martins, G. S., Iozzi, M. A., Martins, M. A., Mattoso, L. H., & Ferreira, F. C. (2004). Caracterização mecânica e térmica de compósitos de poli (cloreto de vinila) reforçados com fibras de sisal. *Polímeros*, *14*, 326–333.

Møller, M. F. (1993). A scaled conjugate gradient algorithm for fast supervised learning. *Neural networks*, *6*(4), 525–533.

Monteiro, S. N., Rodriguez, R. J. S., Lopes, F. P. D., & Sores, B. G. (2013). Efeito da incorporação de fibras de coco no comportamento dinâmico-mecânico de compósitos com matriz poliéster. *Tecnologia em Metalurgia, Materiais e Mineração*, *5*(2), 111–115.

Mwaikambo, L. (2006). Review of the history, properties and application of plant fibres. *African Journal of Science and Technology*, *7*(2), 121.

Nascimento, G., Silva, S., Dias, R., Gomes, I., & Fujiyama. (2019). Estudo e comparação entre compósitos reforçados com fibras naturais, fibras de vidro e híbridos.

Neto, F. L., & Pardini, L. C. (2016). *Compósitos estruturais: ciência e tecnologia*. Editora Blucher.

Oliveira, G. A. B. (2018). *Predição de propriedades mecânicas de compósitos unidirecionais através de redes neurais artificiais* (Unpublished master's thesis). Brasil.

Paixão, R. C. F. d., Penido, R. E.-K., Cury, A. A., & Mendes, J. C. (2022). Comparison of machine learning techniques to predict the compressive strength of concrete and considerations on model generalization. *Revista IBRACON de Estruturas e Materiais*, *15*(5), e15503.

Passatore, C. R. (2013). Química dos polímeros. *Material didático, 3º módulo*.

Pezzolo, D. B. (2019). *Tecidos: história, tramas, tipos e usos*. Editora Senac São Paulo.

Pinto, M. R. O., A Júnior, M. M., Carvalho, L. H., et al. (2005). Influência da adição e da modificação química de uma carga mineral nanoparticulada nas propriedades mecânicas e no envelhecimento térmico de compósitos poliuretano/sisal. *Polímeros*, *15*, 313–319.

Prasad, G. E., Gowda, B. K., & Velmurugan, R. (2017). Comparative study of impact strength characteristics of treated and untreated sisal polyester composites. *Procedia Engineering*, *173*, 778–785.

Recicar, G. L. (2022). Efeito dos processos de laminação manual e laminação termomecânica nas propriedades mecânicas de material compósito carbono-epóxi.

Riedmiller, M., & Braun, H. (1993). *A direct adaptive method for faster backpropagation learning: The rprop algorithm*.

Romão, C. M. N. (2003). Estudo do comportamento mecânico de materiais compósitos de matriz polimérica reforçados com fibras naturais.

Rusell, S. J., & Norvig, P. (2013). *Inteligência artificial. tradução regina célia simille.* Rio de Janeiro: Elsevier.

Schelb, C. G. (2016). Avaliação de tipologias construtivas nos critérios de sustentabilidade: estudo de casos–telhas.

Shepherd, G. M. (2003). *The synaptic organization of the brain*. Oxford university press.

Silva, A. d. N. (2017). Utilização de algoritmo com rede neural artificial na validação de padrões de comportamento do c. elegans.

Silva, A. P. d. O., Quaresma, S., Motta, L., & Francklin, H. (2015). Estudo das propriedades mecânicas de compósitos de matriz epóxi reforçada com fibras de sisal para reforço de estruturas de concreto. In *13º congresso brasileiro de polímeros, natal.*

SILVA, M., P. H. F. (2001). *Fast and accurate neural network gaas mesfet model for time-domain circuit simulation* (Vol. 1).

Silva, S., de Oliveira Neto, S. N., Leite, H. G., de Alcântara, A. E. M., de Oliveira Neto, R. R., & de Souza, G. S. A. (2020). Productivity estimate using regression and artificial neural networks in small familiar areas with agrosilvopastoral systems. *Agroforestry Systems*, *94*, 2081–2097.

Silva, S. O. (2021). Controle de qualidade e desempenho de préimpregnados fibra natu-

ral/epóxi para a produção de compósitos.

Silva, T. L. S., de Oliveira Filho, G. C., & do Nascimento Silva., A. (2024). Finite element analysis of polymeric matrix composites with sisal fiber reinforcement. *JBTH*, *6*(Suppl2), 38–43.

Vasconcelos, J. V. d. B. V. (2013). *Estudo de soluções de baixo impacto ambiental para revestimento têxtil* (Unpublished doctoral dissertation).

Vasiliev, V. V., & Morozov, E. V. (2001). *Mechanics and analysis of composite materials*. Elsevier.

Watt, J. P., Davies, G. F., & O'Connell, R. J. (1976). The elastic properties of composite materials. *Reviews of Geophysics*, *14*(4), 541–563.